Mandelbrot Geometry and Stability in Population Growth Models

IB DP Mathematics Analysis and Approaches HL

Research Question:

How do the period-n bulbs of the Mandelbrot set correspond to stability regions in the bifurcation diagram of the logistic map?

Student number:
Word Count: 4,294

Contents

1 Introduction

The study of nonlinear dynamical systems allows an analysis of real-world phenomena through the lens of abstract mathematics, hence linking together mathematical structure in seemingly unrelated contexts. An example of such connections is the relationship of population dynamics (represented by the logistic map) with the Mandelbrot set.

The Mandelbrot set contains infinitely many regions, called period-n bulbs, where the behaviour of the system repeats itself in cycles of length n. In a similar way, the bifurcation diagram of the logistic map shows stability windows, which are intervals of the growth rate where the system settles into a repeating pattern. The strong visual similarity between these two structures suggests a deeper mathematical correspondence exists between them.

This essay investigates this connection by addressing the Research Question:

> **How do the period-n bulbs of the Mandelbrot set correspond to stability regions in the bifurcation diagram of the logistic map?**

By combining analytical tools, such as conjugacy between dynamical systems, with computational verification of stability intervals, this work aims to demonstrate that the logistic map and the quadratic family are linked through a direct parameter transformation. Establishing such a correspondence not only deepens understanding of the internal structure of these systems, but also highlights how abstract fractal geometry can inform models of population dynamics.

2 Background Information

2.1 Mandelbrot set

2.1.1 Fractals

Fractals are mathematical objects characterised by their self-similarity on different scales; their structure tends to appear regardless of the level of zoom. They are often generated through the iterative application of simple processes, such as a recursive function, resulting in structures with complex and infinite details. The complexity of the details of such structures results in their boundaries being often hard to describe rigorously, which often leads these structures to possess non-integer, or fractional, dimensions [1]. Their connection to dynamic systems make them a central subject in the study of chaos and complexity. [2]

2.1.2 Definition and examples

The Mandelbrot set, first defined in 1979 by Robert W. Brooks and Peter Matelski [2], is a fractal defined as the set of all complex numbers c for which the iteration

$$z_{n+1} = z_n^2 + c, \quad z_0 = 0, \quad (\text{also denoted } P_c(z_n)) \tag{1}$$

remains bounded as $n \to \infty$. [3]. Boundedness in this context is defined as the modulus of z_n (noted $|z_n|$) staying finite. We define the orbit of a number under an iterative application as the sequence of values

$$0, z_1, z_2, z_3, \ldots, z_n,$$

written

$$O(c) = \{z_n\}_{n=0}^{\infty}.$$

We can therefore talk about boundedness as the orbit staying bounded in value. [4]

Looking at the example where $c = -1$, we can apply the Mandelbrot function to it and find:

$$\begin{aligned} z_0 &= 0, \\ z_1 &= 0^2 - 1 = -1, \\ z_2 &= (-1)^2 - 1 = 0, \\ &\ldots \end{aligned} \tag{2}$$

It can be shown that for all $c \in \mathbb{C}$, if there exists some $n > m$ $(n, m \in \mathbb{N})$ such that $z_n = z_m$, c must be part of the Mandelbrot set ($\mathbb{M}$) [5]. In other words, if the orbit of 0 under $f(z) = z^2 + c$ is periodic, then it is bounded, and c is in the Mandelbrot set. In the case where $c = -1$ (2), because the repetition appeared after 2 steps, we say that the orbit of c has a period of 2 and therefore c is part of a period-2 bulb of the Mandelbrot set [6] (The relevance of period-n bulbs in stability analysis of regions of iterative maps such as the logistic map will be seen in Section 4).

In order to apply (1) to complex numbers, it is important to know that the square of a complex number in the form $a + ib$ functions the same way as the square of a binomial. Therefore,

$$(a + ib)^2 = a^2 + 2iab + (ib)^2 = a^2 - b^2 + 2iab \quad (\text{since } i^2 = -1).$$

This being established, we can now analyse the behaviour of the application on complex values of c. Let $c = i + 1$,

$$\begin{aligned} z_0 &= 0 & |z_0| &= 0, \\ z_1 &= 1 + i & |z_1| &= \sqrt{2}, \\ z_2 &= 1 + 3i & |z_2| &= \sqrt{10}, \\ z_3 &= -7 + 7i & |z_3| &= \sqrt{98}, \\ z_4 &= 1 - 97i, \ldots & |z_4| &= \sqrt{94010}, \ldots \end{aligned} \tag{3}$$

Observe that the modulus of z_n does not stay bounded and grows indefinitely, implying that $c = i + 1$ is not part of $\mathbb{M}$.

2.1.3 Visualisation

In order to visualise the Mandelbrot set, the complex plane has to be visibly divided between the points that are part of the set and the ones that are not. This can be done by colouring each point P of the complex plane in white if $P \in \mathbb{M}$, and in black if $P \notin \mathbb{M}$. By doing so around the origin the following structure appears (see Fig.1).

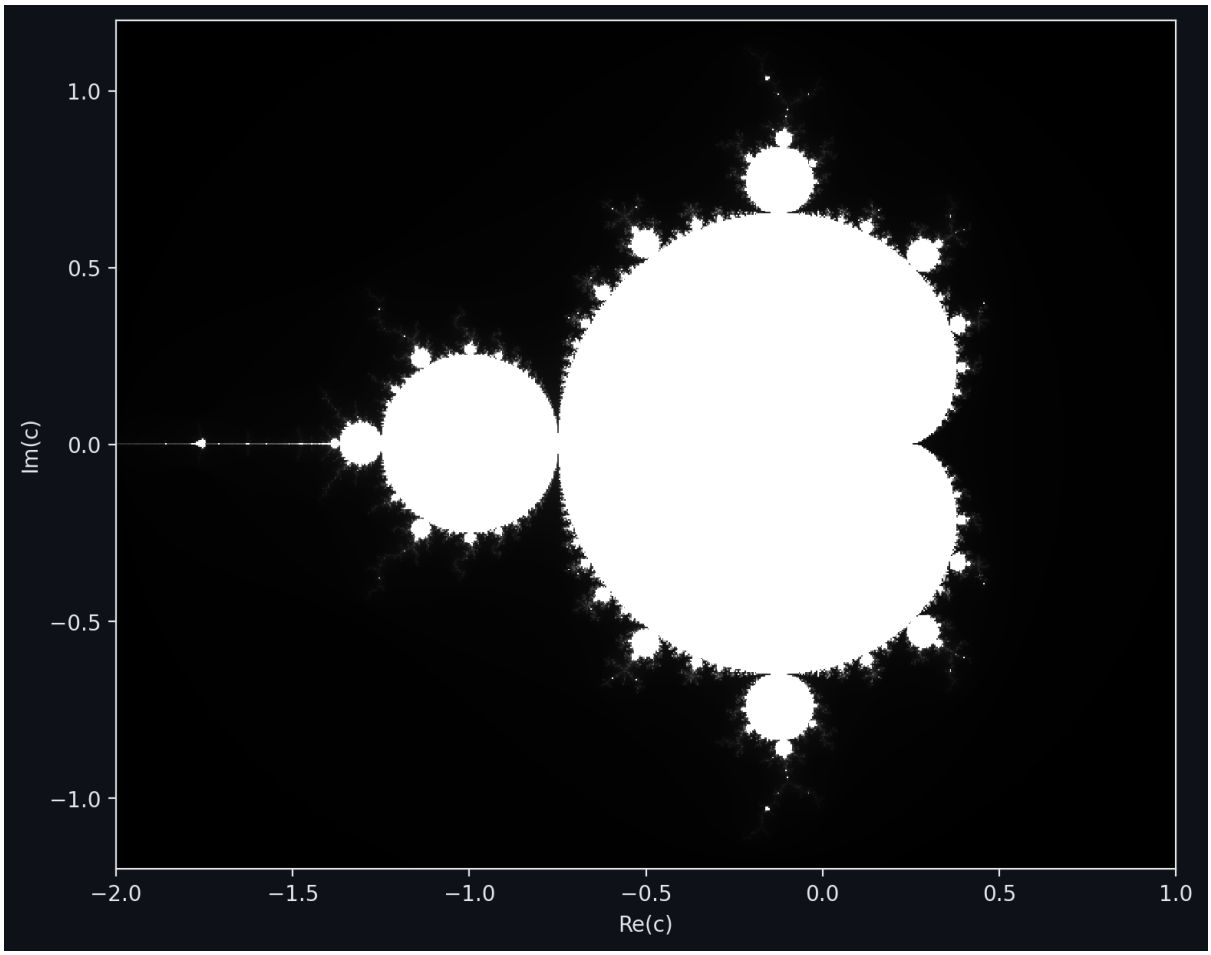

Figure 1: Visualisation of the Mandelbrot set, showing points coloured according to membership in $\mathbb{M}$. (From: author's own visualisation, generated in Python [7])

2.1.4 Hyperbolic components and period-n bulbs

When investigating the structure of the Mandelbrot set, one could look at the orbit of a point c (as done above) but looking at the periodicity of that orbit reveals further important patterns. Regions with the same periodicity, called *hyperbolic components*, form well-defined "bulbs" attached to the main cardioid of the Mandelbrot set (see Fig2).

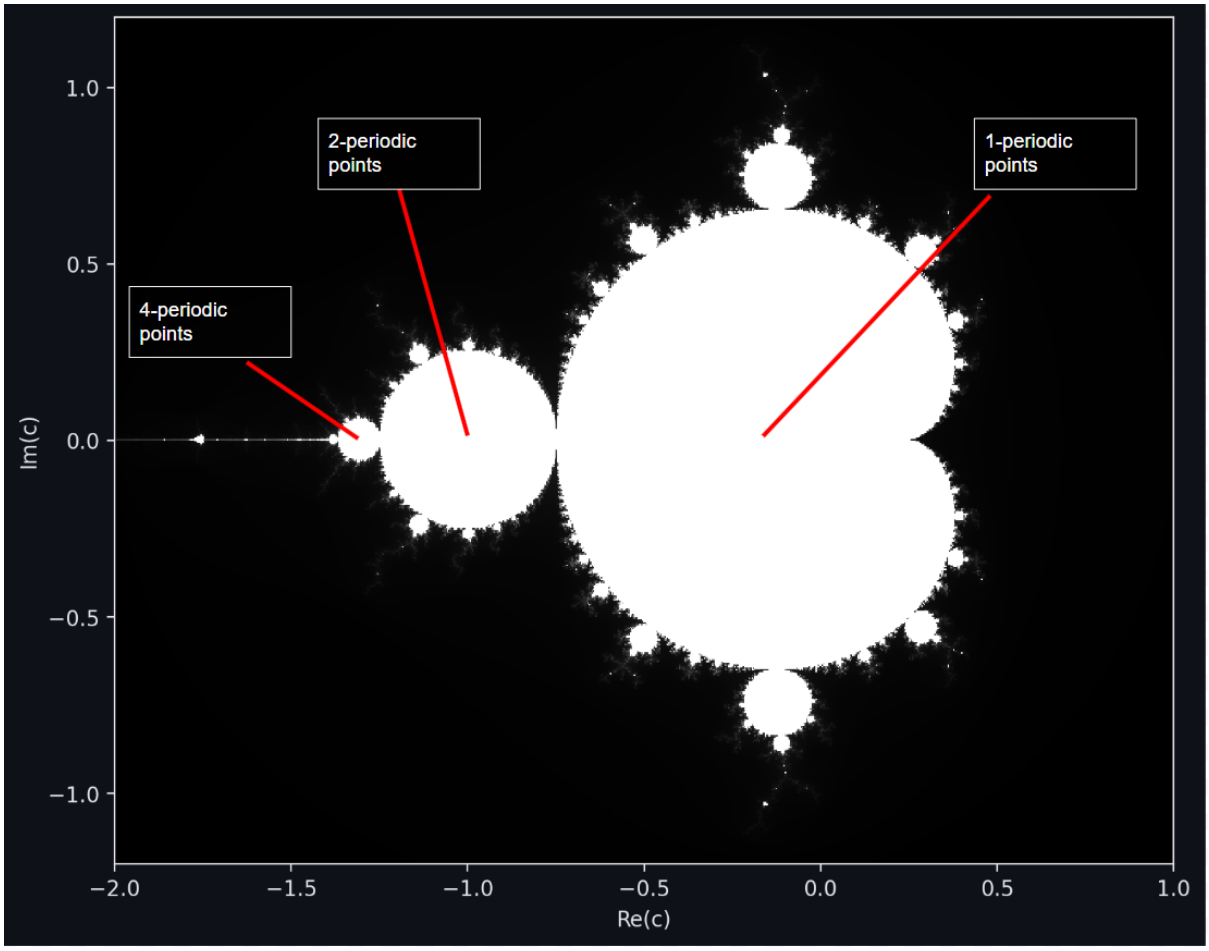

Figure 2: Periodicity of points in the bulbs of the Mandelbrot set, with each bulb labelled by its attracting cycle. From: Author's own visualisation [7]

Definition: A hyperbolic component is a connected region of parameter space for which the repetitive iteration $P_c(z) = z^2 + c$ admits a periodic cycle (called attracting cycle) such as the one in (2) [8] [9] [10]. The reason for their use in this investigation is that these regions are precisely the visible bulbs in Mandelbrot visualisations [6], and they describe where the dynamics are structurally stable [11]. The limitation of such components in the context of the Mandelbrot set is that, on the boundary of a hyperbolic component, the cycle is no longer attracting, which introduces more delicate behaviour which will not be explored in this essay [12].

Each hyperbolic component is labelled by the period of its attracting cycle (see Fig2). The result is the family of period-n bulbs, where each bulb corresponds to parameters c for which the orbit of the critical point ($O(c)$) converges to an attracting cycle of period n [13]. This classification will help visualise how such periodicity in the Mandelbrot set relates to the logistic map.

By introducing the notions of hyperbolic component and period-n bulb, we can now describe the structure of the Mandelbrot set in a way that allows rigorous comparison with the logistic map (2.2). This terminology will be used extensively when addressing the research quesiton of this investigation (4.1).

2.2 Logistic map

2.2.1 Definition and origin

The logistic map is a discrete-time recurrence relation that models the evolution of a population under constrained growth. It is definined as:

$$x_{n+1} = rx_n(1 - x_n) \quad \text{(also denoted } f_r(x_n)\text{)}, \tag{4}$$

where $x_n \in [0, 1]$ represents the normalised population at time step n relative to the maximum sustainable population, or carrying capacity, and $r > 0$ is the growth parameter [14]. In this model, the term x_n accounts for the proportional growth of the population, while $(1-x_n)$ introduces a limiting factor (which could represent real-life limitations like finite resources), hence reducing the growth as x_n approaches the carrying capacity. [15]

The logistic map arises from the logistic growth differential equation,

$$\frac{dP}{dt} = rP(1 - \frac{P}{K}), \tag{5}$$

where P is the population at continuous time t, and K is the carrying capacity, which was first proposed in 1838 by the Belgian mathematician Pierre François Verhulst to describe population growth limited by environmental constraints [16]. In (4), this (5) equation is discretised, giving the logistic map a simpler non-linear iterative model. [17]

While its development was originally aimed towards population modelling, the logistic map was linked to chaos theory in the 1970s, leading to it being studied extensively by mathematicians such as Robert May and Mitchell Feigenbaum [18]. Robert May's 1976 paper demonstrated that varying the parameter r leads to a range of dynamical behaviour; the stability of the system shifting drastically from periodic oscillations to chaos [19]. The sensitivity of the logistic map relates directly to the stability analysis of population growth models. The relationship between the logistic map and stability analysis becomes particularly relevant when attempting to link it to the Mandelbrot set (4.1).

In the context of iterative maps such as (4), we define the period k of a cycle refers to the number of iterations required for the system to return to a previous state. A point x^* has period k if $f_r^{(k)}(x^*) = x^*$ and k is the smallest positive integer with this property, where $f_r^{(k)}$ denotes the value of $f_r(x)$ after k steps [20]. The case $k = 1$ corresponds to fixed points, where the value of the system remains constant over time (see 2.2.2).

2.2.2 Fixed points and stability

For the logistic map (4), a fixed point is a value x^* such that $x_{n+1} = x_n = x^*$. Setting $x_{n+1} = x_n$ in the recurrence gives:

$$x^* = rx^*(1 - x^*) = rx^* - r(x^*)^2$$

$$\therefore 0 = rx^* - r(x^*)^2 - x^*$$

$$\therefore 0 = x^*(r - rx^* - 1) = x^*(r(1 - x^*) - 1)$$

giving two fixed points:

$$x_0^* = 0, \quad x_1^* = 1 - \frac{1}{r}.$$

The *stability* of a fixed point is determined by the derivative of the iteration function

$$f_r(x) = rx(1 - x), \tag{6}$$

evaluated at x^*. A fixed point is stable if

$$|f_r'(x^*)| < 1. \tag{7}$$

This condition (7) follows from linearising the map near x^*: if a small perturbation ϵ_n is applied, the next iteration changes it by approximately $\epsilon_{n+1} \approx f_r'(x^*)\,\epsilon_n$. When $|f_r'(x^*)| < 1$, the perturbation decreases in magnitude over successive iterations, causing trajectories to return to x^*, hence ensuring stability. Conversely, if $|f_r'(x^*)| > 1$, perturbations grow and the fixed point is unstable. [21]

Since

$$f_r'(x) = r(1 - 2x),$$

we have:

- For $x_0^* = 0$: $f_r'(0) = r$. The stability condition $|r| < 1$ implies that the origin is stable for $0 < r < 1$.
- $x_1^* = 1 - \frac{1}{r}$:

$$f_r'\left(1 - \frac{1}{r}\right) = r\left(1 - 2\left(1 - \frac{1}{r}\right)\right) = -r + 2.$$

The stability condition $|-r + 2| < 1$ gives $1 < r < 3$.

Thus:

- For $0 < r < 1$, the population tends to extinction ($x = 0$ stable).
- For $1 < r < 3$, the population approaches the non-zero equilibrium $x = 1 - \frac{1}{r}$.
- At $r = 3$, the fixed point x_1^* loses stability, leading to a *period-doubling bifurcation* (see Section 2.2.3).

These results mark the first stability window in the bifurcation diagram of the logistic map, corresponding to a period-1 region. This can be verified when plotting the bifurcation diagram (see Fig.3):

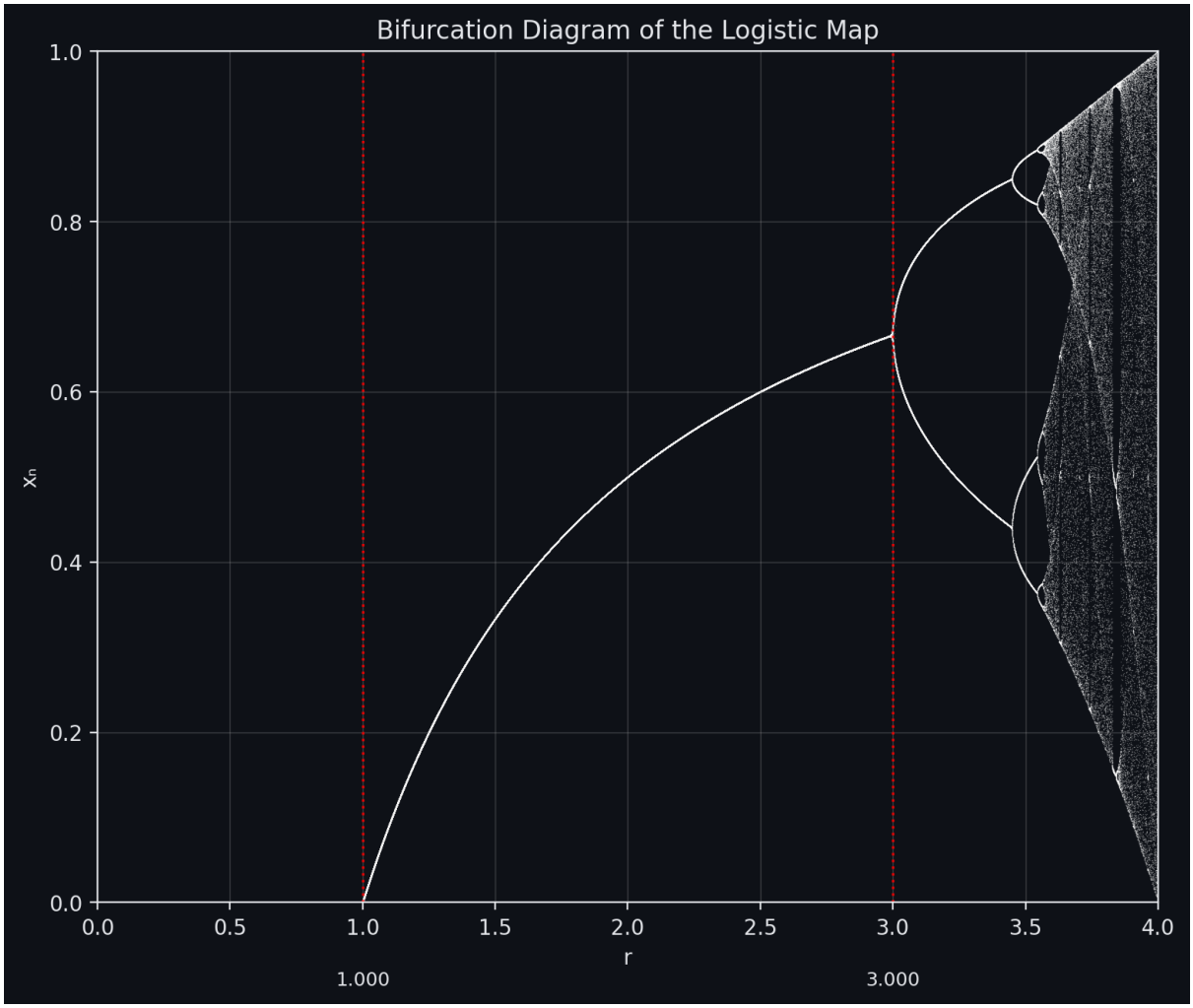

Figure 3: Bifurcation diagram of the logistic map for $1 < r < 3$, showing the period-1 stability window. From: Author's own visualisation [7]

In Fig.3, it can clearly be observed that when $r \in]1, 3[$ the recurrence application settles to one value therefore we call this region of the logistic map a period-1 window.

This periodicity translates, in population dynamics, to the population oscillating between n values as seen in Fig. 4: (a), (b), (c), and (d).

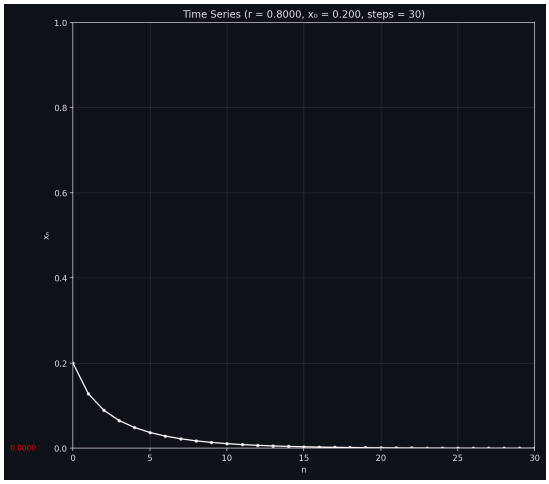

(a) $r = 0.8$, $x_0 = 0.2$ (extinguishing cycle).

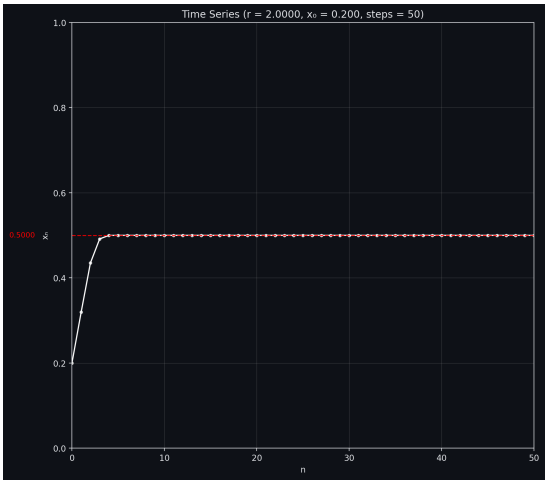

(b) $r = 2.0$, $x_0 = 0.2$ (1-periodic cycle).

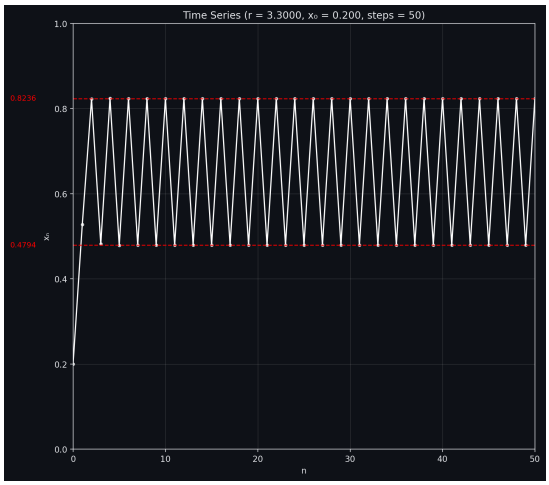

(c) $r = 3.3$, $x_0 = 0.2$ (2-periodic cycle).

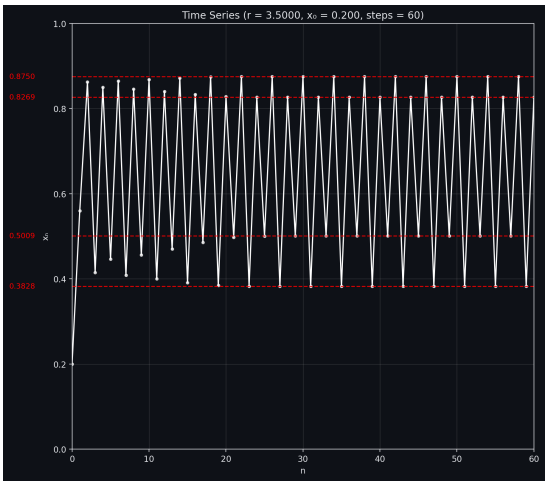

(d) $r = 3.5$, $x_0 = 0.2$ (4-periodic cycle).

Figure 4: Time series plots of the logistic map for different parameter values r, starting from $x_0 = 0.2$. Each trajectory x_n converges to a stable periodic orbit, illustrated by red dashed lines indicating the attracting cycle values. Panel (a) shows the population extinguishing after a certain number of steps, (b) shows the population converging to a fixed point (1-periodic cycles), while (c) and (d) show the population converging to higher-order periodic cycles (2-periodic and 4-periodic respectively). From: Author's own visualisation [7].

2.2.3 Period-doubling and the bifurcation diagram

When the growth rate parameter r is increased beyond $r = 3$, the fixed point

$$x_1^* = 1 - \frac{1}{r}$$

loses stability [22]. This is because at $r = 3$, we have

$$x_1^* = \frac{2}{3}$$

$$\therefore |f_r'(x_1^*)| = 1$$

This indicates the beginning of a bifurcation. Rather than converging to a single value, the population oscillates between two distinct values, therefore the region following $r = 3$ is a period-2 region. This marks the first example of a period-doubling bifurcation, where the system's attractor changes from period k to period $2k$. [23] [24] [25]

Definition: A periodic attractor is the set of values towards which a system tends to evolve after many iterations, regardless of the initial conditions. In the context of the logistic map, the attractor may be a single fixed point, a finite cycle of period n, or, for larger values of r, a chaotic set [26] [27]. The attractor therefore represents the long-term behaviour of the system.

The logistic map exhibits a cascade of such bifurcations as r increases:

1. At $r = 3.000$, the stable period-1 point bifurcates to period-2 (2.2.3) (see Fig.5).
2. At $r = 1 + \sqrt{6} \approx 3.449$, the period-2 cycle bifurcates to period-4 (2.2.3) (see Fig.6).
3. Subsequent doublings occur more rapidly, with the intervals between bifurcation values shrinking geometrically, converging to the **Feigenbaum point** [28]

$$r_\infty \approx 3.569946\ldots,$$

beyond which the system enters chaos [29] [30].

The ratio of successive differences in bifurcation parameters,

$$\delta \;=\; \lim_{n\to\infty} \frac{r_n - r_{n-1}}{r_{n+1} - r_n},$$

is a universal constant ($\delta \approx 4.6692$) [25], independent of the specific form of the quadratic map. This universality links the logistic map to other nonlinear dynamical systems, including the quadratic polynomial $f_c(z) = z^2 + c$ underlying the Mandelbrot set [31] [32].

Stability windows appear as horizontal bands containing a finite set of points (periodic attractors), separated by chaotic regions. The period-n windows of the bifurcation diagram have a direct relation to the period-n bulbs of the Mandelbrot set as will be shown in 4.1.

3.2.4 Example calculations for small periods

The values of r that generate k-periodic cycles (with prime periods k, $k > 1$) of the logistic map as r goes beyond 3 can be found when solving for r [33]:

$$f_r^{(k)}(x^*) = x^*, \quad f_r(x^*) \neq x^*. \tag{8}$$

A cycle is said to have prime period k if k is the smallest positive integer such that

$$f_r^{(k)}(x^*) = x^*,$$

while no smaller $(m < k) \in \mathbb{N}$ satisfies $f_r^{(m)}(x^*) = x^*$. In other words, a prime period-k cycle consists of k distinct points visited in order by the map, and the orbit does not close up after fewer than k iterations [34].

Period-2 cycle. A point x^* belongs to a period-2 cycle (has a prime period of $k = 2$) if it satisfies:

$$f_r^{(2)}(x^*) = f_r(f_r(x^*)) = x^*, \quad f_r(x^*) \neq x^*.$$

Expanding,

$$f_r(x) = rx(1-x),$$
$$f_r^{(2)}(x) = f_r(rx(1-x)) = r\big(rx(1-x)\big)\Big(1 - rx(1-x)\Big).$$

So the equation becomes

$$r^2x(1-x)(1-rx+rx^2) = x.$$

Rearranging gives a cubic equation whose solutions include the fixed points (period-1), while the other two correspond to the genuine period-2 orbit. Solving explicitly gives:

$$x_{1,2} = \frac{r+1 \pm \sqrt{(r-3)(r+1)}}{2r}.$$

This pair is stable when

$$\left|(f_r^{(2)})'(x^*)\right| < 1,$$

which holds for $3 < r < 1 + \sqrt{6} \approx 3.449$. This interval corresponds to the period-2 stability window observed in the bifurcation diagram (see Fig.5).

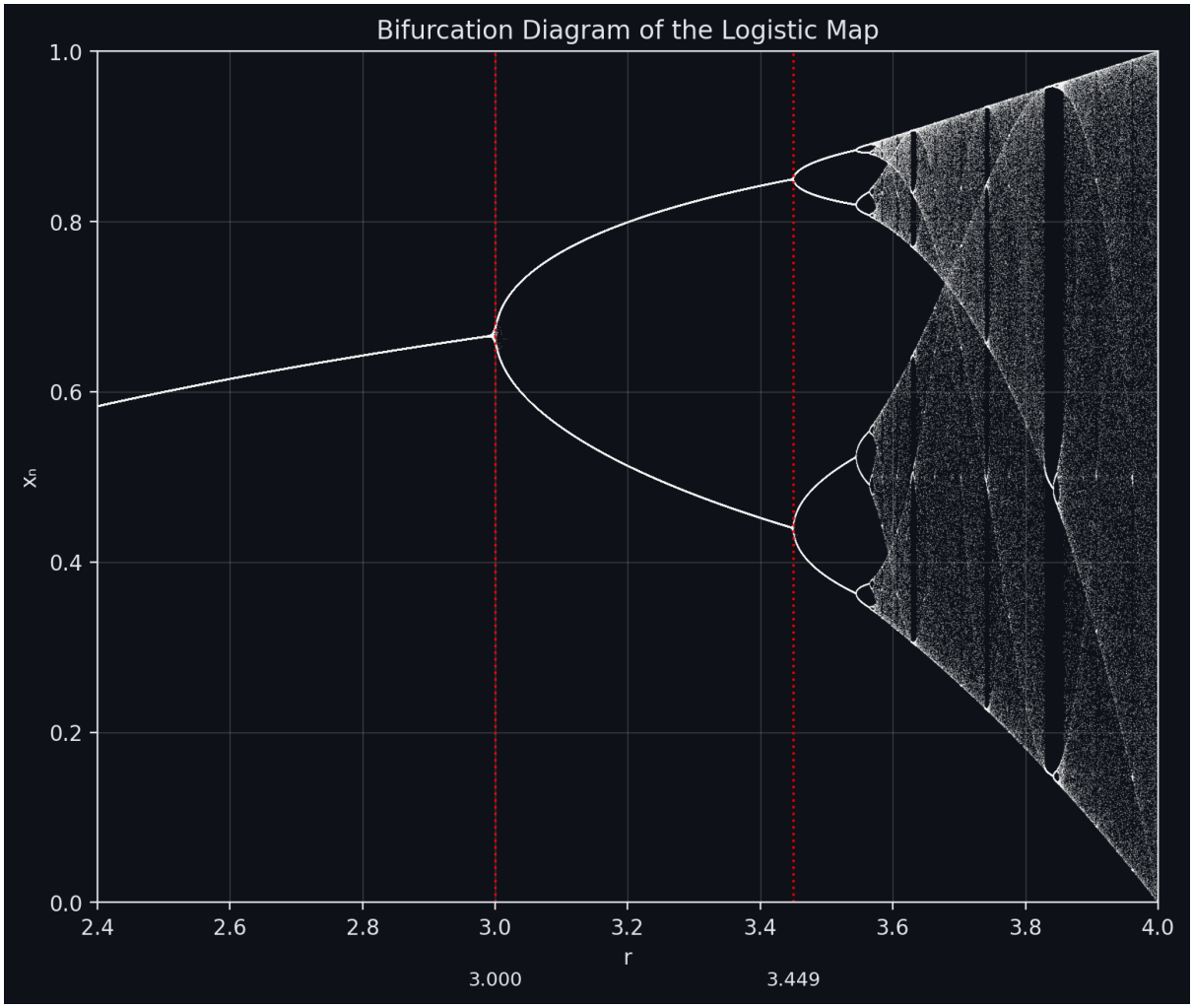

Figure 5: Bifurcation diagram of the logistic map for $3 < r < 1 + \sqrt{6}$, showing the period-2 stability window. From: Author's own visualisation [7]

Period-4 cycle. Similarly, a period-4 point satisfies

$$f_r^{(4)}(x^*) = x^*, \quad f_r^{(k)}(x^*) \neq x^* \text{ for } k < 4.$$

To evaluate solutions (x^*) for this expression, let us first write the 2-iteration function:

$$g(x) = f_r^{(2)}(x) = r^2 x(1-x)(1-rx+rx^2).$$

Therefore, a point has period 4 if

$$g^{(2)}(x^*) = x^*,$$

but $g(x^*) \neq x^*$ (not period 2) and $f_r(x^*) \neq x^*$ (not period 1).

The equation $g(g(x)) - x = 0$ expands to a polynomial of degree 16. We can simplify it by noting that some solutions correspond to period-1 and period-2 cycles, and factoring them out, the remaining roots give the period-4 cycle. The exact algebraic expressions are extremely complicated [35], so we do not write them here.

Stability. A 4-cycle $\{x_0, x_1, x_2, x_3\}$ is stable when

$$\left|(f_r^{(4)})'(x_0)\right| < 1.$$

We know,

$$f_r(x) = r\,x(1-x) \text{ and } x_{j+1} = f_r(x_j), \quad j = 0,1,2,3, \quad (x_4 = x_0).$$

$$\begin{aligned}
\therefore (f_r^{(2)})'(x_0) &= (f_r \circ f_r)'(x_0) = f_r'\big(f_r(x_0)\big) \cdot f_r'(x_0) = f_r'(x_1)\, f_r'(x_0), \\
\therefore (f_r^{(3)})'(x_0) &= \big(f_r \circ f_r^{(2)}\big)'(x_0) = f_r'\big(f_r^{(2)}(x_0)\big) \cdot (f_r^{(2)})'(x_0) = f_r'(x_2)\,\big[f_r'(x_1)\, f_r'(x_0)\big], \\
\therefore (f_r^{(4)})'(x_0) &= \big(f_r \circ f_r^{(3)}\big)'(x_0) = f_r'\big(f_r^{(3)}(x_0)\big) \cdot (f_r^{(3)})'(x_0) \\
&= f_r'(x_3)\,\big[f_r'(x_2)\, f_r'(x_1)\, f_r'(x_0)\big] \\
&= \prod_{j=0}^{3} f_r'(x_j).
\end{aligned}$$

Taking absolute values,

$$\big|(f_r^{(4)})'(x_0)\big| \;=\; \prod_{j=0}^{3} \big|f_r'(x_j)\big|.$$

Since $f_r'(x) = r(1-2x)$, this becomes

$$\big|(f_r^{(4)})'(x_0)\big| \;=\; \prod_{j=0}^{3} \big|\, r(1-2x_j)\,\big| \;=\; |r|^4 \prod_{j=0}^{3} \big|1-2x_j\big| < 1 \tag{9}$$

We call this stability condition the *multiplier condition* [36], we often denote it $|\Lambda| < 1$.

This condition gives the range of r values where a 4-cycle appears. The 4-cycle first appears exactly when the period-2 cycle becomes unstable, which happens at

$$r = 1 + \sqrt{6} \approx 3.449.$$

It remains stable until the next bifurcation at

$$r \approx 3.544.$$

Therefore, the period-4 cycle exists and is stable for

$$\boxed{3.449 < r < 3.544}.$$

Within this interval [37], the logistic map cycles between 4 point as observes on the bifurcation digram (see Fig.6).

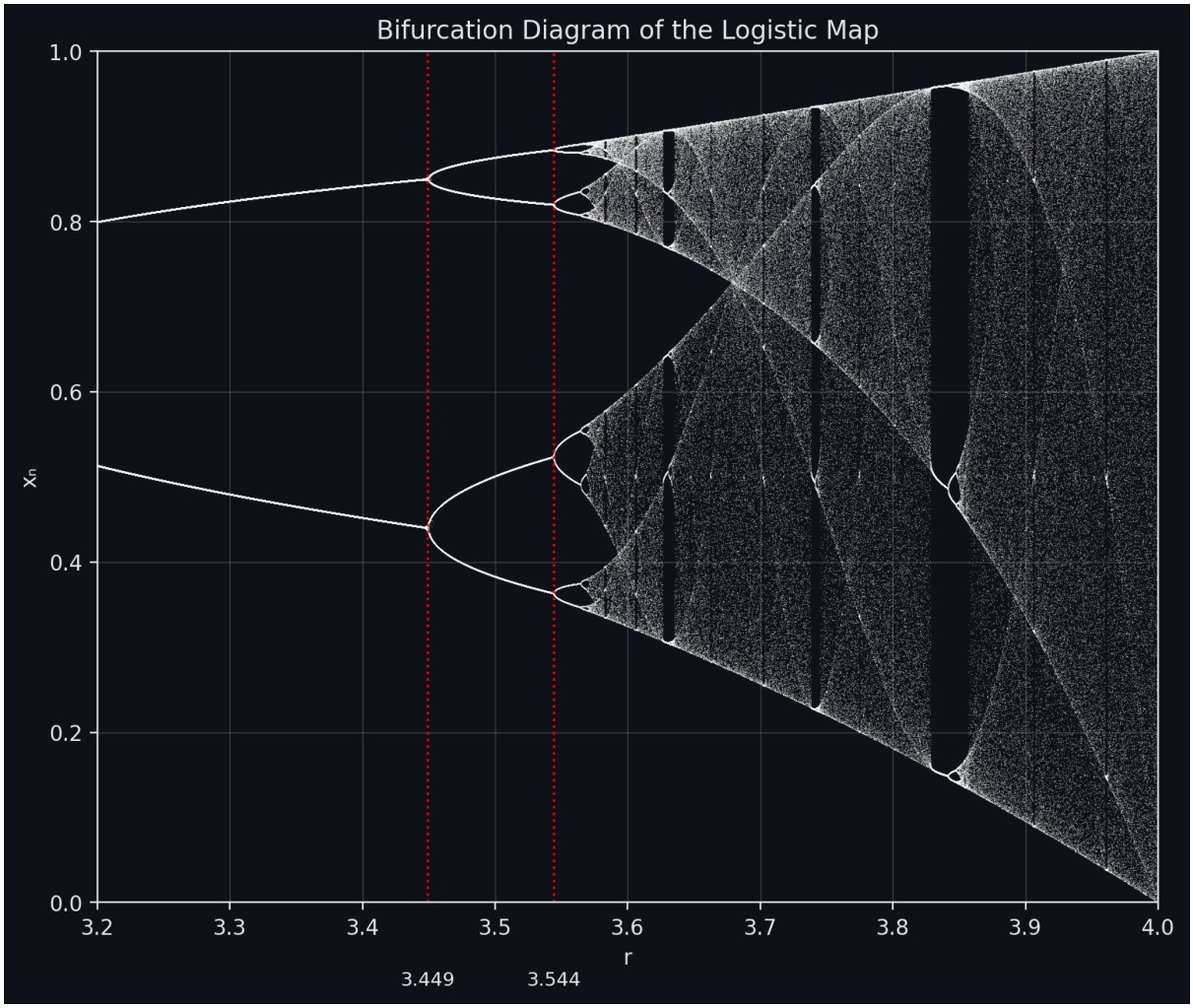

Figure 6: Bifurcation diagram of the logistic map for $3.449 < r < 3.544$, showing the period-4 stability window. From: Author's own visualisation [7], 2025)

The same process can be followed for larger k-periodic cycles.

The main limitation of the multiplier condition is that it only detects local stability. At bifurcation points, where the multiplier equals ± 1 [38], convergence of the orbits towards the cycle becomes arbitrarily slower, making stability harder to determine numerically [39]. This becomes a particularly relevant problem when computing stability for higher values of k. Making it harder to link the bifurcation structure of the logistic map to the bulbs in the Mandelbrot set.

3 Methodology

3.1 Hypotheses

Null hypothesis. There is no systematic correspondence between the period-n bulbs of the Mandelbrot set and the stability windows of the logistic map; any resemblance is accidental.

Research hypothesis. The period-n bulbs of the Mandelbrot set correspond directly to the period-n stability windows of the logistic map, such that each bulb predicts a parameter interval of stable cycles in the bifurcation diagram.

Strategy. To test these hypotheses, this paper will construct and apply an explicit conjugacy between the logistic family and the quadratic family. If the research hypothesis is correct, then the conjugacy should map logistic stability windows (with centers and boundaries) to the corresponding Mandelbrot bulbs on the real slice.

3.2 Analytical approach

Exploring conjugacy is appropriate in this investigation as it preserves the two essential invariants of the systems under study: periodicity and multipliers. As these quantities determine the location of stability regions in the logistic map and the structure of bulbs in the Mandelbrot set, conjugacy provides a rigorous framework for transferring analytical results about cycles, centers, and boundaries between the two families.

Explicit conjugacy and parameter map. For each $r \in \mathbb{R}$ define

$$T(x) = 1 - 2x, \quad S_r(y) = \tfrac{r}{2}y, \quad \Phi_r = S_r \circ T, \quad \psi(r) = \tfrac{r(2-r)}{4}.$$

We then show the conjugacy

$$\Phi_r \circ f_r = P_{\psi(r)} \circ \Phi_r,$$

so periods and multipliers are preserved under Φ_r. Key consequences:

1. A point is period k for f_r iff its image is period k for $P_{\psi(r)}$.
2. Multipliers coincide: $(f_r^{\,k})'(x^*) = (P_{\psi(r)}^{k})'(z^*)$.
3. The logistic critical point $x = \frac{1}{2}$ maps to $z = 0$, hence centers of stability windows (where $f_r^{\,n}(\frac{1}{2}) = \frac{1}{2}$) correspond exactly to Mandelbrot bulb centers (where $P_c^{\,n}(0) = 0$).
4. Window endpoints given by $\left|(f_r^{\,k})'(x^*)\right| = 1$ map to parabolic bulb boundary points $\left|(P_c^{\,k})'(z^*)\right| = 1$ on the real slice.

Explicit cases used.

- **Period–1:** $1 < r < 3$ with center $r = 2$ maps to the main cardioid real slice $-\frac{3}{4} < c < \frac{1}{4}$ with center $c = 0$.
- **Period–2:** $3 < r < 1 + \sqrt{6}$, center $r = 1 + \sqrt{5}$, maps to the period-2 bulb slice $-\frac{5}{4} < c < -\frac{3}{4}$ with center $c = -1$.
- **Higher periods:** centers are given by $f_r^{\,k}(\frac{1}{2}) = \frac{1}{2}$ (prime period k) and mapped via $c = \psi(r)$. Endpoints are solutions of $\left|(f_r^{\,k})'(x^*)\right| = 1$, obtained numerically for $k \geq 4$.

Scope. All results are restricted to the real slice $c = \psi(r) \in \mathbb{R}$.

3.3 Numerical approach

Computing stability intervals, centers, and endpoints in the logistic map, and mapping them via $c = \psi(r)$, allows to confirm the claims made in the analysis part, therefore, helping address the research hypothesis along the real slice. The calculations will consist of 2 main checks:

Interval mapping. For each period-k stability window of the logistic map, the multiplier condition $|(f_r^k)'(x^*)| < 1$ is applied to determine the stability interval in r. These intervals are then mapped through $c = \psi(r)$ to identify the corresponding slices of the Mandelbrot set. Similarly, window endpoints where $|(f_r^k)'(x^*)| = 1$ are mapped to parabolic points on the boundary of the corresponding bulb.

Center mapping. Centers are found by solving $f_r^k(\frac{1}{2}) = \frac{1}{2}$ for prime periods k, and verified against $P_c^k(0) = 0$ to confirm the correspondence of superattracting centers.

Limitations. Numerical detection loses in precision as $|\Lambda| \to 1$, where stability changes occur, therefore, endpoints are reported with a set precision of $\pm 10^{-5}$.

3.4 Computational approach

In addition to hand calculations, I developed two interactive Python programs to visualise and experiment with the systems studied:

- A **logistic map explorer**, which generates bifurcation diagrams, cobweb plots, and time series trajectories for chosen values of r. It also allows cycle detection and stability marking, confirming the analytical and numerical intervals.
- A **Mandelbrot explorer**, capable of zooming, colour-mapping, and high-precision rendering, used to visualise the geometry of hyperbolic components and their centers. The zoom and iteration controls allow for visualisation of the fractal structures contained within the Mandelbrot set.

Screenshots of both interfaces are provided in the Appendices, together with a GitHub repository link containing the full code and usage instructions. These computational tools extend the investigation by producing accurate diagrams and visualisations, enabling comparisons between logistic stability windows and Mandelbrot bulbs beyond what is feasible through manual calculation alone.

4 Analysis

4.1 Connection between Logistic Map and Mandelbrot Set

4.1.1 Definitions

Maps.

Let X be a set (in this essay, $X \subseteq \mathbb{R}$ or $X \subseteq \mathbb{C}$). A *map* (or function) is a rule $f : X \to X$ that assigns to each $x \in X$ a value $f(x) \in X$ [40].

Conjugacy.

A *conjugacy* between two dynamical systems implies essentially equivalent systems under a change of coordinates. We define it as follows:

Let $f : X \to X$ and $g : Y \to Y$ be maps. We say that f and g are *conjugate* if there exists an invertible change of coordinates $h : X \to Y$ (a bijection, i.e. a one-to-one and onto correspondence) such that [41]

$$h \circ f = g \circ h.$$

If h is affine (linear plus shift), we say f and g are *affinely conjugate* [42]. Conjugacy preserves the structure of the dynamics, in particular the existence, period, and stability of cycles. This makes it possible to transfer results from one system to another [43]. Therefore, proving conjugacy between the logistic map and the Mandelbrot set will be crucial in demonstrating the link between the hyperbolic components of the Mandelbrot set and the logistic map.

Superattraction.

A cycle is called "superattracting" if and only if it contains a critical point $z = 0$, making the multiplier

$$\left|(f_r^{(4)})'(x_0)\right| \;=\; \prod_{j=0}^{3} \left| r(1-2x_j) \right| \;=\; |r|^4 \prod_{j=0}^{3} \left|1-2x_j\right| = 0$$

Therefore, forcing convergence to the k-periodic cycle [44].

Critical points.

For a differentiable map $f(x)$, a *critical point* is a value x_c where the derivative:

$$f'(x_c) = 0.$$

The *critical orbit* is the sequence $\{f^n(x_c)\}_{n\geq 0}$. In one-dimensional iterative maps, the orbit of the critical point is decisive because if it converges to a cycle, that cycle is attracting [45].

Center.

The *center* of a hyperbolic component of the Mandelbrot set is the parameter value c for which the associated attracting cycle is superattracting. [10]

4.1.2 Criteria for conjugacy

Looking at the connection between the logistic map and the Mandelbrot set will be done through showing conjugacy between the two systems.

We now introduce two parallel criteria that allow a rigorous comparison between the logistic map and the quadratic family:

- For the logistic family $f_r(x) = r\,x(1-x)$, a *period-k stability window* is an r-interval on which there exists an attracting cycle of prime period k. Such a cycle is found by the periodic-point equation

$$f_r^{(k)}(x^*) = x^* \quad \text{(with prime period } k\text{)},$$

and the *multiplier* (stability) condition

$$\left|(f_r^{(k)})'(x^*)\right| = \prod_{j=0}^{k-1} \left|f_r'(x_j)\right| = \prod_{j=0}^{k-1} \left|r(1-2x_j)\right| < 1,$$

where $x_{j+1} = f_r(x_j)$ along the cycle.

- For the quadratic family $P_c(z) = z^2 + c$, a *period-n bulb* (hyperbolic component) consists of the parameters c for which there exists an attracting n-cycle. The *center* of the bulb is characterised by a *superattracting* n-cycle,

$$P_c^{(n)}(x^*) = 0 \quad \text{and} \quad P_c^{(m)}(x^*) \neq 0 \text{ for } m < n.$$

The criteria above establish a rigorous bridge between the two systems by showing a conjugacy between the two (see 4.1.3). By constructing a parameter map and an affine conjugacy, we can transfer period and stability information directly from the logistic map to the quadratic family, thereby explaining the correspondence between period-n stability windows of the logistic map and the period-n bulbs of the Mandelbrot set. In this essay, the connection between the logistic map and the quadratic family is restricted to real parameters due to the way the logistic map is defined ($r \in \mathbb{R}$). However, the Mandelbrot set is defined over the full complex plane, so the correspondence we obtain is exact only along the real slice. Expanding this link over the complex numbers can however be done, providing a good extension of this essay.

4.1.3 A parameter conjugacy linking f_r and P_c.

Analytical demonstration of conjugacy.

For each fixed $r \in \mathbb{R}$, define the affine maps

$$T(x) = 1 - 2x, \qquad S_r(y) = \tfrac{r}{2}y, \qquad \Phi_r = S_r \circ T.$$

We can attempt to transform the logistic map into a quadratic family to create a conjugacy.

Starting from $f_r(x) = rx(1-x)$, we compute

$$\begin{aligned} T\big(f_r(x)\big) &= 1 - 2rx(1-x) \\ &= 1 - \tfrac{r}{2}\big(1 - T(x)^2\big) \\ &= \tfrac{r}{2}T(x)^2 + \Big(1 - \tfrac{r}{2}\Big). \end{aligned}$$

Applying S_r gives

$$\begin{aligned} \Phi_r\big(f_r(x)\big) &= S_r\big(\tfrac{r}{2}T(x)^2 + 1 - \tfrac{r}{2}\big) \\ &= \big(S_r(T(x))\big)^2 \; + \; \tfrac{r}{2}\Big(1 - \tfrac{r}{2}\Big). \end{aligned}$$

A quadratic family has emerged under a transformation of r that we define

$$\psi(r) = \frac{r(2-r)}{4}.$$

The previous identity becomes

$$\Phi_r \circ f_r(x) \;=\; \big(\Phi_r(x)\big)^2 + \psi(r).$$

We therefore obtain the affine conjugacy

$$\boxed{\Phi_r \circ f_r = P_{\psi(r)} \circ \Phi_r} \qquad \text{with} \qquad P_c(z) = z^2 + c.$$

Hence, for each fixed r, the logistic map f_r is affinely conjugate to the quadratic polynomial $P_{\psi(r)}$ under the change of variables Φ_r. Note that this conjugacy only relates the *real slice* of the parameter space, since $\psi(r) \in \mathbb{R}$. Phenomena involving complex parameters $c \notin \mathbb{R}$ lie beyond this correspondence.

Consequences.

Let x^* be a prime period-k point of f_r and $z^* = \Phi_r(x^*)$. Then

$$\Phi_r\big(f_r^{(k)}(x^*)\big) = \Phi_r(x^*) \quad \Longleftrightarrow \quad P_{\psi(r)}^{(k)}(z^*) = z^*,$$

so z^* is a period-k point for $P_{\psi(r)}$. Moreover, differentiating the conjugacy $\Phi_r \circ f_r^{(k)} = P_{\psi(r)}^{(k)} \circ \Phi_r$ and using that Φ_r is affine (constant nonzero derivative) gives

$$(P_{\psi(r)}^{(k)})'(z^*) = (f_r^{(k)})'(x^*).$$

Hence multipliers are identical: a cycle is attracting/neutral/repelling for f_r if and only if the corresponding cycle is so for $P_{\psi(r)}$. Hence it can be said that the stability of both systems is equal. However equality of multipliers does not imply equality of geometric shape of attractors, only their local stability type. Therefore:

> For each k, the set of parameters r for which f_r has an attracting period-k cycle maps under $c = \psi(r)$ onto the set of parameters c for which P_c has an attracting period-k cycle. In particular, each logistic stability window of period k corresponds to a period-k bulb of the Mandelbrot set (restricted to the real slice of parameter space via $c = \psi(r)$).

Limitation. The correspondence between period-k windows and period-k bulbs holds along the real slice $c = \psi(r)$, but it does not describe the full structure of the Mandelbrot set. Each period-k bulb is organised around a superattracting k-cycle at its center, yet its interior also contains further bifurcations $k \to 2k \to 4k \to \cdots$ and other dynamics that are not visible from the one-dimensional logistic bifurcation diagram. This is seen in Fig.7 where hyperbolic components of doubling period are seen outside of the real slice (where the imaginary component of c satisfies $\Im(c) \neq 0$).

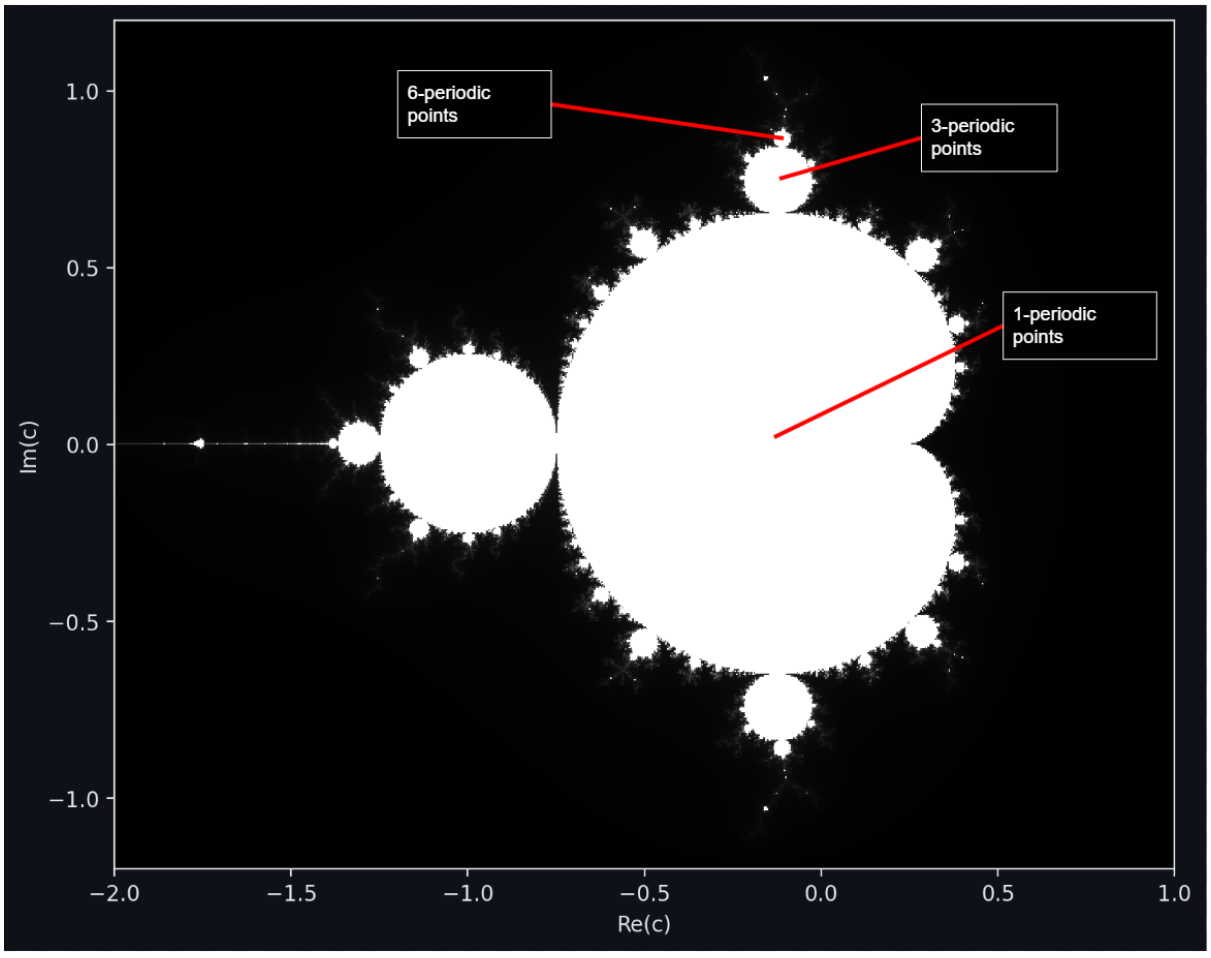

Figure 7: Annotated Mandelbrot set showing bulbs of different periodicity, with examples of 1-, 3-, and 6-periodic points indicated. From: Author's own visualisation [7]

This limitation is a lot clearer in the following image from Adam Cunningham (see Fig.8).

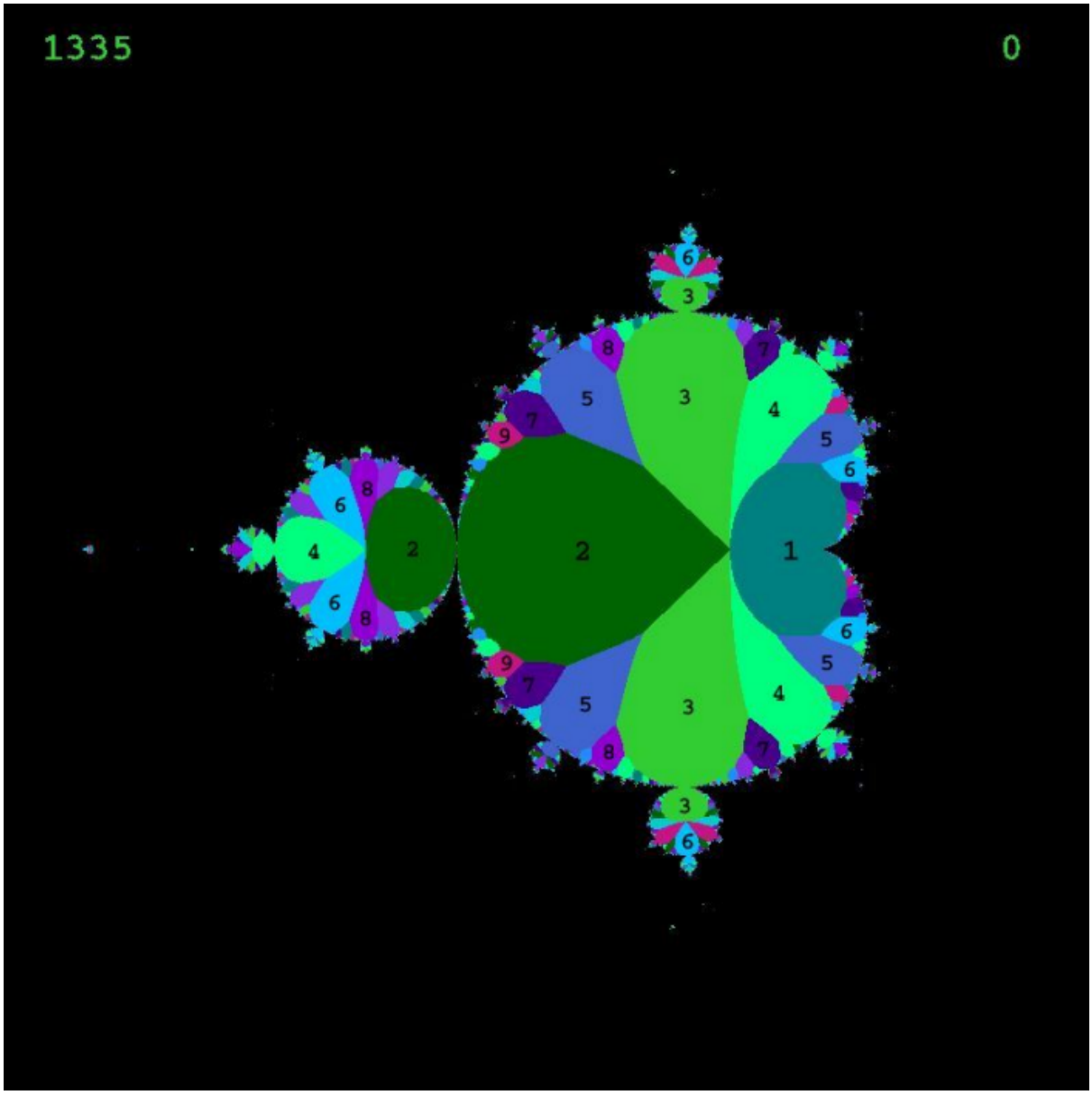

Figure 8: Orbit cycle map of the Mandelbrot set, showing the internal partition of the set into distinct hyperbolic components labelled by the period of the attracting cycle. Each coloured region corresponds to parameters c for which P_c converges to a cycle of the labelled period. From: Cunningham, A. (2013), *Displaying the Internal Structure of the Mandelbrot Set*, State University of New York at Buffalo. [46]

Moreover, away from the real axis, the boundaries of these bulbs are surrounded by disconnected bulbs, refered to as satellite bubls and are essentially smaller Mandelbrot sets (see Fig.9), as well as other bulbs with varied internal angles. Thus, the period-k label captures the real-slice correspondence but not the other fractal substructures off the real line.

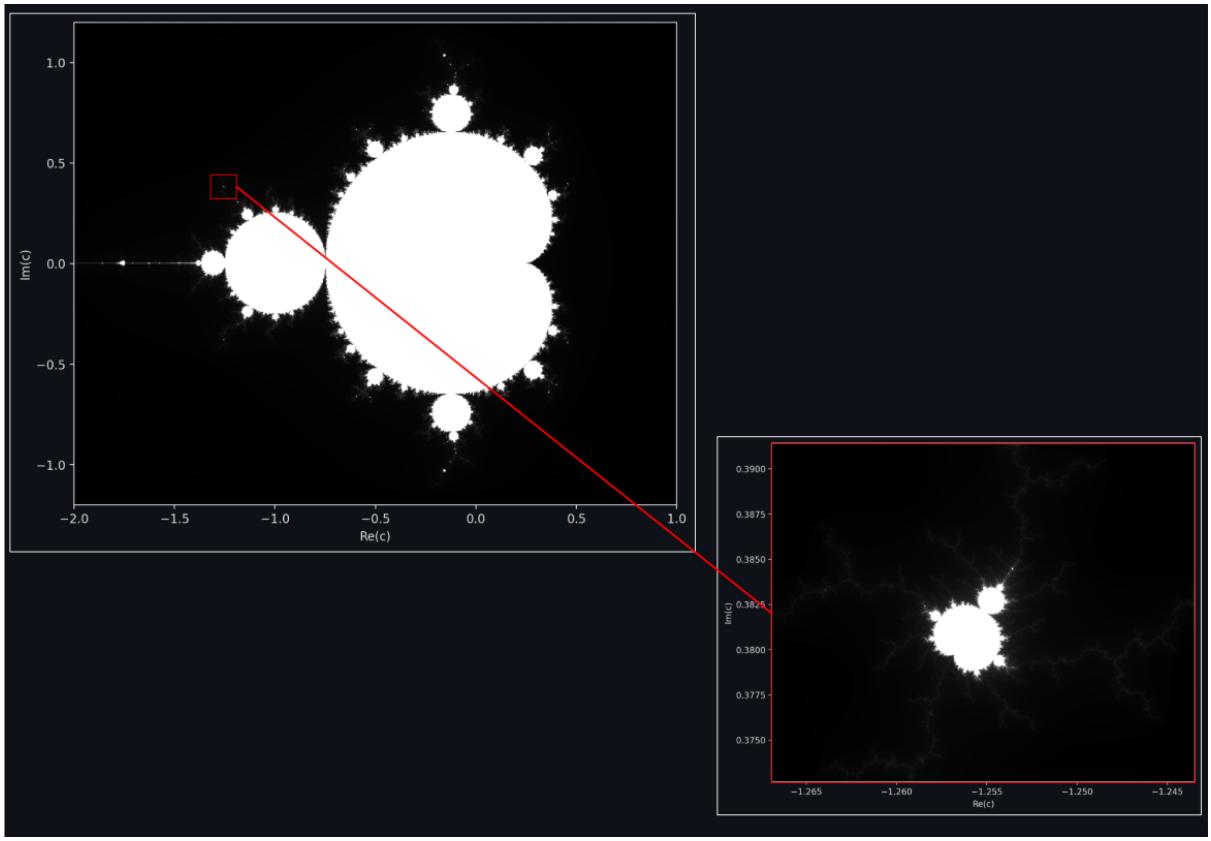

Figure 9: Zoom into a satellite copy of the Mandelbrot set. The left panel shows the full set with the selected region marked in red, while the right panel illustrates the magnified satellite structure, which replicates the overall form of the Mandelbrot set. From: Author's own visualisation [7]

4.2 Computational Correspondences and Calculations

To confirm the results obtained in 4.1.3, we now compute the exact transforms for the first stability windows and their corresponding bulbs, verifying that their boundaries and centers coincide. Throughout these calculations we restrict attention to the real slice of the Mandelbrot set; accordingly, references to 'cardioids' or other hyperbolic components of the Mandelbrot set are to be interpreted as referring only to their intersections with the real axis.

4.2.1 Period-1

Stability interval mapping.

The nonzero fixed point of f_r is $x^* = 1 - \frac{1}{r}$ with multiplier

$$f_r'(x^*) = r(1 - 2x^*) = r\Big(1 - 2 + \tfrac{2}{r}\Big) = 2 - r.$$

Similarly, the fixed points of P_c are solutions of

$$z^* = (z^*)^2 + c.$$

For such a fixed point, the multiplier is

$$(P_c)'(z^*) = 2z^* = 2 \cdot \frac{1 \pm \sqrt{1 - 4c}}{2} = 1 \pm \sqrt{1 - 4c}.$$

The stability condition $|2 - r| < 1$ gives $1 < r < 3$. Under the mapping $c = \psi(r) = \frac{r(2-r)}{4}$, the endpoints map to

$$r = 1 \;\mapsto\; c = \tfrac{1}{4}, \qquad r = 3 \;\mapsto\; c = -\tfrac{3}{4}.$$

At the right endpoint $c = \frac{1}{4}$ the fixed point becomes neutral with multiplier $+1$; at the left endpoint $c = -\frac{3}{4}$ the multiplier is -1. The mapped endpoints are therefore precisely the endpoints of the real slice of the main cardioid ($c \in (-\frac{3}{4}, \frac{1}{4})$).

Center mapping.

The superattracting fixed point for f_r occurs when $f_r(\frac{1}{2}) = \frac{1}{2}$, i.e.

$$\frac{r}{4} = \frac{1}{2} \implies r = 2, \qquad c = \psi(2) = 0.$$

This, $c = 0$ being the center of the main cardioid ($P_0(z_n) = 0,$ with $z_0 = 0$), confirms a center-to-center correspondence over the first periodicity window.

4.2.2 Period-2

Stability interval mapping.

A period-2 window begins when the period-1 fixed point loses stability: $r = 3 \mapsto c = -\frac{3}{4}$. The period-2 window persists until the period-2 cycle becomes neutral ($r = 1 + \sqrt{6}$), mapping under ψ gives

$$r = 1 + \sqrt{6} \;\mapsto\; c = \psi(1 + \sqrt{6}) = \frac{(1 + \sqrt{6})(2 - (1 + \sqrt{6}))}{4} = -\frac{5}{4}.$$

Thus the real slice of the period-2 bulb is the interval $c \in (-\frac{5}{4}, -\frac{3}{4})$, matching the known interval for the period-2 bulb [47].

Center mapping.

Solve $f_r^{(2)}(\frac{1}{2}) = \frac{1}{2}$ with $f_r(\frac{1}{2}) \neq \frac{1}{2}$:

$$f_r\Big(\tfrac{1}{2}\Big) = \frac{r}{4}, \qquad f_r^{(2)}\Big(\tfrac{1}{2}\Big) = r \cdot \frac{r}{4}\Big(1 - \frac{r}{4}\Big) = \frac{r^2}{4}\Big(1 - \frac{r}{4}\Big).$$

Set $f_r^{(2)}(\frac{1}{2}) = \frac{1}{2}$:

$$\frac{r^2}{4}\Big(1 - \frac{r}{4}\Big) = \frac{1}{2} \quad \Longleftrightarrow \quad 4r^2 - r^3 - 8 = 0 \quad \Longleftrightarrow \quad (r - 2)(r^2 - 2r - 4) = 0.$$

Reject $r = 2$ (period 1). Hence $r = 1 + \sqrt{5} \approx 3.23607$, and

$$c = \psi(1 + \sqrt{5}) = \frac{(1 + \sqrt{5})(2 - (1 + \sqrt{5}))}{4} = \frac{(1 + \sqrt{5})(1 - \sqrt{5})}{4} = \frac{1 - 5}{4} = -1,$$

the center of the 2-periodic bulb. As expected, the cycle includes $x = \frac{1}{2}$, so the multiplier is 0. Therefore a center-to-center maping can also be done here.

4.2.3 Mapping table.

The same process can be followed for further periods and the results found are as follows (to 5 s.f.):

Period	Logistic window in r	center r	Image in $c = \psi(r)$ (real slice)
1	$1 < r < 3$	$r = 2$	$-\frac{3}{4} < c < \frac{1}{4}$, center $c = 0$
2	$3 < r < 1 + \sqrt{6}$	$r = 1 + \sqrt{5}$	$-\frac{5}{4} < c < -\frac{3}{4}$, center $c = -1$
4	$1 + \sqrt{6} < r \lesssim 3.54409$	$r \approx 3.49856$	$-1.36810 \lesssim c < -\frac{5}{4}$, center $c \approx -1.31070$
8	$3.54408 \lesssim r \lesssim 3.56428$	$r \approx 3.55464$	$-1.39389 \lesssim c < -1.36809$, center $c \approx -1.38155$
16	$3.56428 \lesssim r \lesssim 3.56871$	$r \approx 3.56667$	$-1.39957 \lesssim c < -1.39389$, center $c \approx -1.39695$
...	...	...	...

4.3 Scope, assumptions, and limitations

(i) Local stability: The multiplier test ($|\Lambda| < 1$) is a strictly local criterion, valid only in a neighbourhood of the cycle. Near the boundary (when $|\Lambda| = 1$), convergence becomes arbitrarily slow and orbits become extremely long before stabilising, making the stability harder to notice numerically. Numerically, this manifests as apparent "chaos" or ambiguous period classification, since finite-precision as well as finite iteration depth are used, it causes an attracting cycle to appear unstable, or vice versa. These difficulties are increased for higher-period cycles and when attempting to resolve bifurcation thresholds to high precision.

(ii) Prime-period detection: When solving $f_r^{(k)}(x) = x$ algebraically, the equation also admits solutions corresponding to lower-period cycles that divide k. Without additional filtering, this would lead to false positives where a period-k cycle is reported even though the orbit actually repeats after fewer steps. To address this, we remove lower-period factors and then apply numerical period tests modulo all smaller divisors of k to confirm the orbit is of prime period k. This dual procedure reduces misclassification, but is computationally more expensive for larger k and does not entirely eliminate sensitivity to numerical tolerances, so prime-period labels near bifurcation points remain approximate.

(iii) Measure-zero exceptions: Certain parameter values, such as Misiurewicz points [48] where the critical orbit is preperiodic, do not fall inside stability windows but instead lie precisely on their boundaries or within chaotic regions. These points form sets of (Lebesgue) measure zero, meaning they occupy no interval in parameter space and do not affect the correspondence between windows and bulbs. Nevertheless, they introduce local irregularities: near such parameters, cycles can appear to destabilise abruptly, and numerical classification becomes ambiguous. Their existence highlights that the window–bulb correspondence is exact only at the level of attracting cycles, while boundary and chaotic dynamics require finer tools beyond the scope of this essay.

4.4 Conclusion

We have established the following correspondences between the logistic map and the quadratic family:

1. **Parameter map and conjugacy.** We derived an explicit parameter transformation

   $$c = \psi(r) = \tfrac{r(2-r)}{4},$$

   together with an affine conjugacy Φ_r such that $\Phi_r \circ f_r = P_c \circ \Phi_r$. This shows that the logistic family and the quadratic family are dynamically equivalent along the real parameter slice.

2. **Preservation of stability.** Because Φ_r is affine, multipliers of corresponding cycles are equal. This means that attracting, neutral, and repelling behaviour in the logistic map transfers exactly to the quadratic family. Thus the classification of stability windows in r is equivalent to the classification of hyperbolic components in c.

3. **Critical orbit and centers.** The logistic critical point $x = \frac{1}{2}$ maps directly to $z = 0$ (the critical point of P_c). Since superattracting cycles contain the critical orbit, the condition $f_r^{(n)}(\frac{1}{2}) = \frac{1}{2}$ corresponds to $P_c^{(n)}(0) = 0$. Hence the centers of logistic stability windows map to the centers of the Mandelbrot bulbs, as confirmed for periods 1, 2, 4, 8, and 16 in our computations.

4. **Boundaries of windows and bulbs.** Stability boundaries occur where the multiplier has modulus one: $|(f_r^{(k)})'(x^*)| = 1$ or equivalently $|(P_c^{(k)})'(z^*)| = 1$. Under the parameter map, the logistic bifurcation thresholds align with the boundary points of the Mandelbrot bulbs. Therefore demonstrating that the endpoints of windows correspond across the two systems.

Therefore, the period-n stability windows of the logistic map correspond, under $c = \psi(r)$, to the period-n bulbs of the Mandelbrot set. This correspondence follows from the affine conjugacy and preservation of multipliers, aligning centers, interiors, and boundaries for each period. The correspondence is exact on the real slice and at the level of periods/multipliers. However, the different geometric structures outside the real axis require complex analytical tools beyond the scope of this essay.

References

[1] Fractal Foundation, "What Are Fractals?" https://fractalfoundation.org/resources/what-are-fractals/, accessed: 2025-08-17.

[2] K. Falconer, *Fractals: A Very Short Introduction*. Oxford: Oxford University Press, 2013.

[3] J. C. P. Campuzano and B. S. Chongchitmate, "5.5: The Mandelbrot Set," Mathematics LibreTexts, 2025, accessed: 2025-08-17. [Online]. Available: https://math.libretexts.org/Bookshelves/Analysis/Complex_Analysis_-_A_Visual_and_Interactive_Introduction_(Ponce_Campuzano)/05%3A_Chapter_5/5.05%3A_The_Mandelbrot_Set

[4] E. R. Miranda and A. Escalante, *Computer Sound Design: Synthesis Techniques and Programming*, 2nd ed. Oxford, UK: Newnes/Elsevier, 2001, chapter 4: Iterative algorithms, chaos, and fractals. Accessed: 2025-08-17.

[5] M. Burkey, "Structure in Chaos: An Exploration into the Mandelbrot Set," Whitman College, Walla Walla, WA, 2023, accessed: 2025-08-17. [Online]. Available: https://arminda.whitman.edu/_flysystem/fedora/2023-08/Structure_in_chaos_an_exploration_into_the_Mandelbrot_set.pdf

[6] R. L. Devaney, "The Complex Geometry of the Mandelbrot Set," Lecture notes, Prague, 2013, accessed: 2025-08-17. [Online]. Available: http://math.bu.edu/people/bob/papers/prague.pdf

[7] M. Susskind, "Mandelbrot-LogisticMap-EE (code repository)," GitHub, 2024–2025, accessed: 2025-08-17. [Online]. Available: https://github.com/matanou/Mandelbrot-LogisticMap-EE

[8] L. Keen and J. Kotus, "Dynamics of the family $\lambda \tan z$," *Conformal Geometry and Dynamics of the American Mathematical Society*, vol. 1, pp. 28–57, 1997.

[9] F. Monard, "Math 207 – spring '17 – lecture 20: Introduction to complex dynamics – mandelbrot and friends," Lecture notes, 2017.

[10] J. Milnor, "Hyperbolic components," Institute for Mathematical Sciences, Stony Brook University, Tech. Rep. IMS12-02, 2012, accessed: 19 Aug. 2025. [Online]. Available: https://www.math.stonybrook.edu/preprints/ims12-02.pdf

[11] C. Heiland-Allen, "Patterns in Embedded Julia Sets," mathr.co.uk (blog), 2017, accessed: 2025-08-17. [Online]. Available: https://mathr.co.uk/blog/2017-11-06_patterns_in_embedded_julia_sets.html

[12] A. Chéritat, "Computer-generated Math Pictures and Animation — Galerie I: Fractals," Personal website, Université de Toulouse, 2016, accessed: 2025-08-17. [Online]. Available: https://www.math.univ-toulouse.fr/~cheritat/wiki-draw/index.php/Mandelbrot_set

[13] E. Dummit, "Dynamics, Chaos, and Fractals (Part 5): Introduction to Complex Dynamics," Course notes, Math 3543, Northeastern University, 2023, accessed: 2025-08-17. [Online]. Available: https://dummit.cos.northeastern.edu/teaching_su23_3543/dynamics_5_introduction_to_complex_dynamics_v2.00.pdf

[14] E. W. Weisstein, "Logistic map," From MathWorld–A Wolfram Web Resource, 2024, accessed: 2025-08-14. [Online]. Available: https://mathworld.wolfram.com/LogisticMap.html

[15] G. Strang and E. Herman, "8.4: The logistic equation," Mathematics LibreTexts, 2024, accessed: 2025-08-14. [Online]. Available: https://math.libretexts.org/Bookshelves/Calculus/Calculus_(OpenStax)/08%3A_Introduction_to_Differential_Equations/8.04%3A_The_Logistic_Equation

[16] P. F. Verhulst, "Notice sur la loi que la population suit dans son accroissement," *Correspondance Mathématique et Physique*, vol. 10, pp. 113–121, 1838.

[17] G. Boeing, "Chaos Theory and the Logistic Map," Geoff Boeing Blog, 2015, accessed: 2025-08-17. [Online]. Available: https://geoffboeing.com/2015/03/chaos-theory-logistic-map/

[18] S. Lee, "Logistic Map Dynamics Explained," Number Analytics Blog, 2025, accessed: 2025-08-17. [Online]. Available: https://www.numberanalytics.com/blog/ultimate-guide-logistic-map-dynamical-systems

[19] R. M. May, "Simple mathematical models with very complicated dynamics," *Nature*, vol. 261, no. 5560, pp. 459–467, 1976.

[20] Nathaniel, "The Logistic Map," nathaniel.ai, n.d., accessed: 2025-08-17. [Online]. Available: https://www.nathaniel.ai/logistic-map/

[21] J. R. Chasnov, "8.1: Fixed points and stability," https://math.libretexts.org/Bookshelves/Differential_Equations/Differential_Equations_%28Chasnov%29/08%3A_Nonlinear_Differential_Equations/8.01%3A_Fixed_Points_and_Stability, Nov. 2021, accessed: 2025-08-16.

[22] F. Franco-Medrano, "Stability and chaos in real polynomial maps," *ResearchGate*, Jun. 2013, accessed: 2025-08-16. [Online]. Available: https://www.researchgate.net/publication/266026010_Stability_and_chaos_in_real_polynomial_maps

[23] A. Menasri, "Generalized logistic map and its applications," *AIP Advances*, vol. 15, no. 3, Mar. 2025, accessed: 2025-05-01. [Online]. Available: https://doi.org/10.1063/5.0263704

[24] A. Quillen, "PHY256 Lecture Notes on Bifurcations and Maps," https://astro.pas.rochester.edu/~aquillen/phy256/lectures/bif_maps.pdf, 2021, accessed: 2025-05-01.

[25] S. Bullett, "The Logistic Map, Period-doubling and Universal Constants," Lecture notes, Queen Mary University of London, accessed: 2025-08-17. [Online]. Available: https://webspace.maths.qmul.ac.uk/s.r.bullett/cf_chapter3.pdf

[26] Fiveable, "3.3 types of attractors – chaos theory," https://library.fiveable.me/chaos-theory/unit-3/types-attractors/study-guide/THSUlEJENrwcpgvX, 2024, accessed: 2025-08-16.

[27] J. Guo, "Analysis of chaotic systems," Oct. 2014, university of Chicago, Accessed: 2025-08-16.

[28] D. Kartofelev, "Lecture Notes 11 – Nonlinear Dynamics and Feigenbaum Constants," Tallinn University of Technology (YFX1560 course), 2013, accessed: 2025-08-17. [Online]. Available: https://www.tud.ttu.ee/web/dmitri.kartofelev/YFX1560/LectureNotes_11.pdf

[29] B. Luque, L. Lacasa, F. Ballesteros, and A. Robledo, "Analytical properties of horizontal visibility graphs in the feigenbaum scenario," *Chaos: An Interdisciplinary Journal of Nonlinear Science*, vol. 22, no. 1, p. 013109, Jan. 2012, accessed: 2025-08-17. [Online]. Available: https://arxiv.org/abs/1201.2514

[30] D. Tong, "2 discrete time," https://www.damtp.cam.ac.uk/user/tong/mathbio/mathbio2.pdf, accessed: 2025-08-16.

[31] A. G. Doz, "Theoretical-heuristic derivation sommerfeld's fine structure constant by feigenbaum's constant (delta): Periodic logistic maps of double bifurcation," https://vixra.org/pdf/1705.0355v2.pdf, Jun. 2017, accessed: 2025-08-16.

[32] R. O'Farrell, "Renormalization and universality in dynamics," https://math.uchicago.edu/~may/REU2024/REUPapers/O'Farrell.pdf, 2024, unpublished REU report; accessed: 2025-08-16.

[33] Wikipedia Contributors, "Logistic map," Wikipedia, Wikimedia Foundation, 2019, accessed: 2025-08-17. [Online]. Available: https://en.wikipedia.org/wiki/Logistic_map

[34] Y. Vorobets, "Math 614 dynamical systems and chaos," 2016, texas A&M University, Lecture notes.

[35] G. Rukavina, "Quadratic recurrence equations - exact explicit solution of period four fixed points functions in bifurcation diagram," arXiv:0802.2565 [math.DS], 2008, accessed: 2025-08-17. [Online]. Available: https://arxiv.org/abs/0802.2565

[36] P. Cvitanović, R. Artuso, R. Mainieri, G. Tanner, and G. Vattay, *Chaos: Classical and Quantum*, version 17 ed. Niels Bohr Institute, Copenhagen, 2017, chapter 5: Cycle Stability, Example 5.1, pp. 103–114. [Online]. Available: https://chaosbook.org/version17/chapters/invariants-2p.pdf

[37] University of Southampton, "Lecture 7 – logistic map and period doubling," 2012, lecture notes.

[38] R. Ghaziani, "Bifurcations of maps: Numerical algorithms and applications," Ph.D. dissertation, Ghent University, Ghent, Belgium, 2010.

[39] J. Sanders *et al.*, "Numerical bifurcation analysis of differential equations," 1985, accessed: 2025-08-17. [Online]. Available: https://webspace.science.uu.nl/~kouzn101/NBA/nba.pdf

[40] J. K. Hunter, "Index of /~hunter/intro_analysis_pdf," https://www.math.ucdavis.edu/~hunter/intro_analysis_pdf, 2015, accessed: 19 Aug. 2025.

[41] J. Marklof and C. Ulcigrai, "Dynamical systems and ergodic theory," https://people.maths.bris.ac.uk/~ip13935/dyn/CorinnaII.pdf, 2015, accessed: 19 Aug. 2025.

[42] A. Avila, M. Lyubich, and W. de Melo, "Regular or stochastic dynamics in real analytic families of unimodal maps," *Inventiones Mathematicae*, vol. 154, no. 3, pp. 451–550, 2003, accessed: 19 Apr. 2024. [Online]. Available: https://www.math.stonybrook.edu/preprints/ims01-15.pdf

[43] C. Ulcigrai, *Dynamical Systems and Ergodic Theory Part I: Examples of Dynamical Systems*. University of Zurich, Department of Mathematics, 2018, accessed: 19 Aug. 2025.

[44] A. Levy, "An algebraic proof of thurston's rigidity for maps with a superattracting cycle," 2014, accessed: 19 Aug. 2025. [Online]. Available: https://people.kth.se/~alonlevy/rigidity4.pdf

[45] L. Rempe, "Holomorphic dynamics, lecture iv," January 2008, accessed: 19 Aug. 2025. [Online]. Available: https://pcwww.liv.ac.uk/~lrempe/workshops/liv_jan_08/liverpool

[46] A. Cunningham, "Displaying the internal structure of the mandelbrot set," State University of New York at Buffalo, Tech. Rep., 2013, numerical Analysis MTH 537. [Online]. Available: https://www.acsu.buffalo.edu/~adamcunn/downloads/MandelbrotSet.pdf

[47] M. Lyubich, "On the dynamics of quadratic polynomials: Hyperbolicity and holomorphic motions," https://arxiv.org/abs/math/9201282, 1992, arXiv, Cornell University Library. Accessed 17 Aug. 2025.

[48] R. L. Devaney. (2022, May) 6.2: Misiurewicz points and the m-set self-similarity. Accessed: 2025-08-20. [Online]. Available: https://math.libretexts.org/Bookshelves/Scientific_Computing_Simulations_and_Modeling/The_Mandelbrot_and_Julia_sets_Anatomy_(Demidov)/6%3A_Periodic_and_preperiodic_points/6.2%3A_Misiurewicz_points_and_the_M-set_self-similarity

Appendices

Appendix A: Code Repository

The full source code for the logistic map and Mandelbrot visualisation tools developed for this essay is available on GitHub:

`https://github.com/matanou/Mandelbrot-LogisticMap-EE`

Instructions for running the programs are included in the repository's `README.md` file.

Appendix B: Logistic Map Explorer Interface

(i) Bifurcation Diagram Explorer

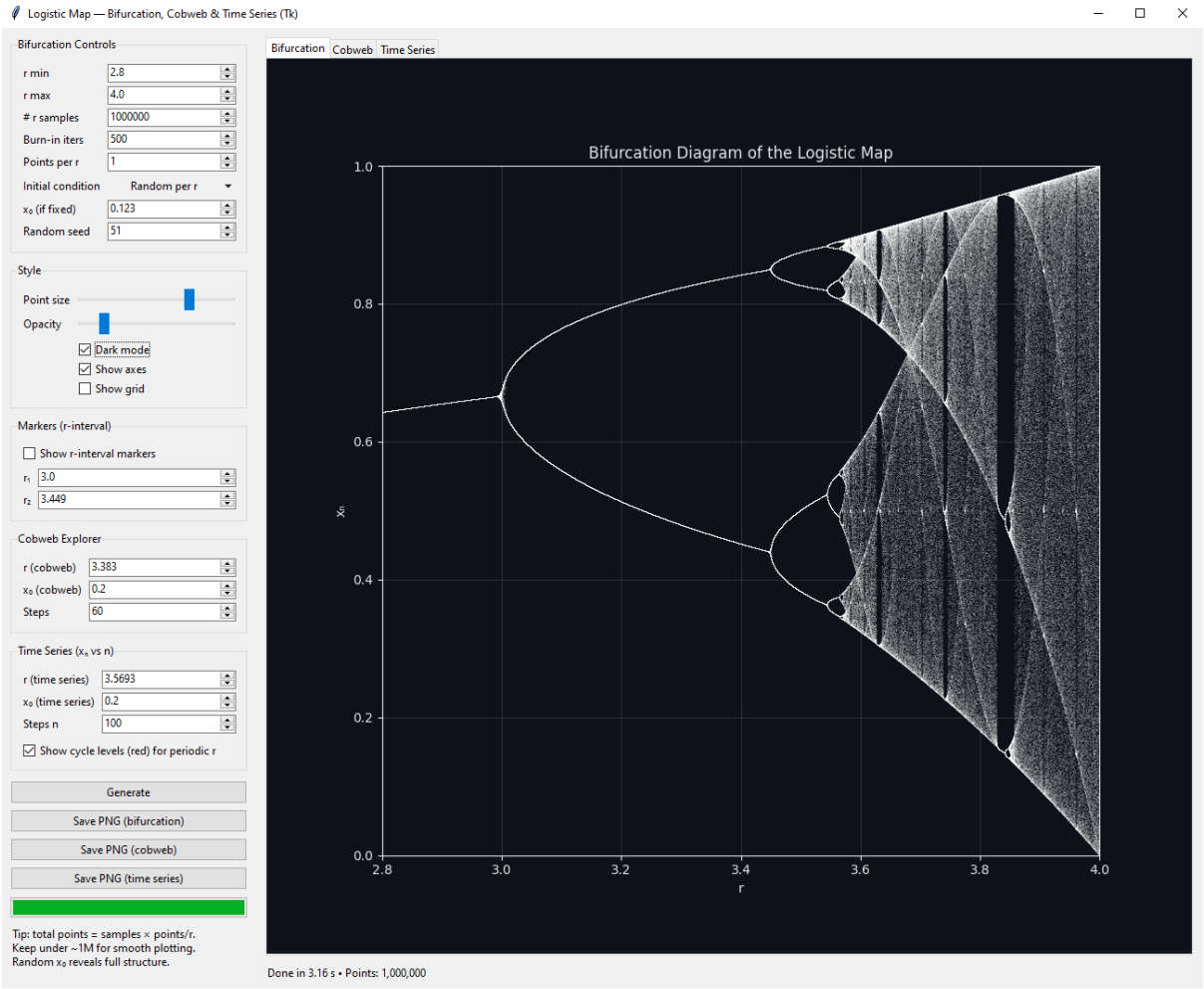

Figure 10: Screenshot of the logistic map explorer GUI, showing bifurcation diagram and parameter controls.

(ii) Time Series Explorer

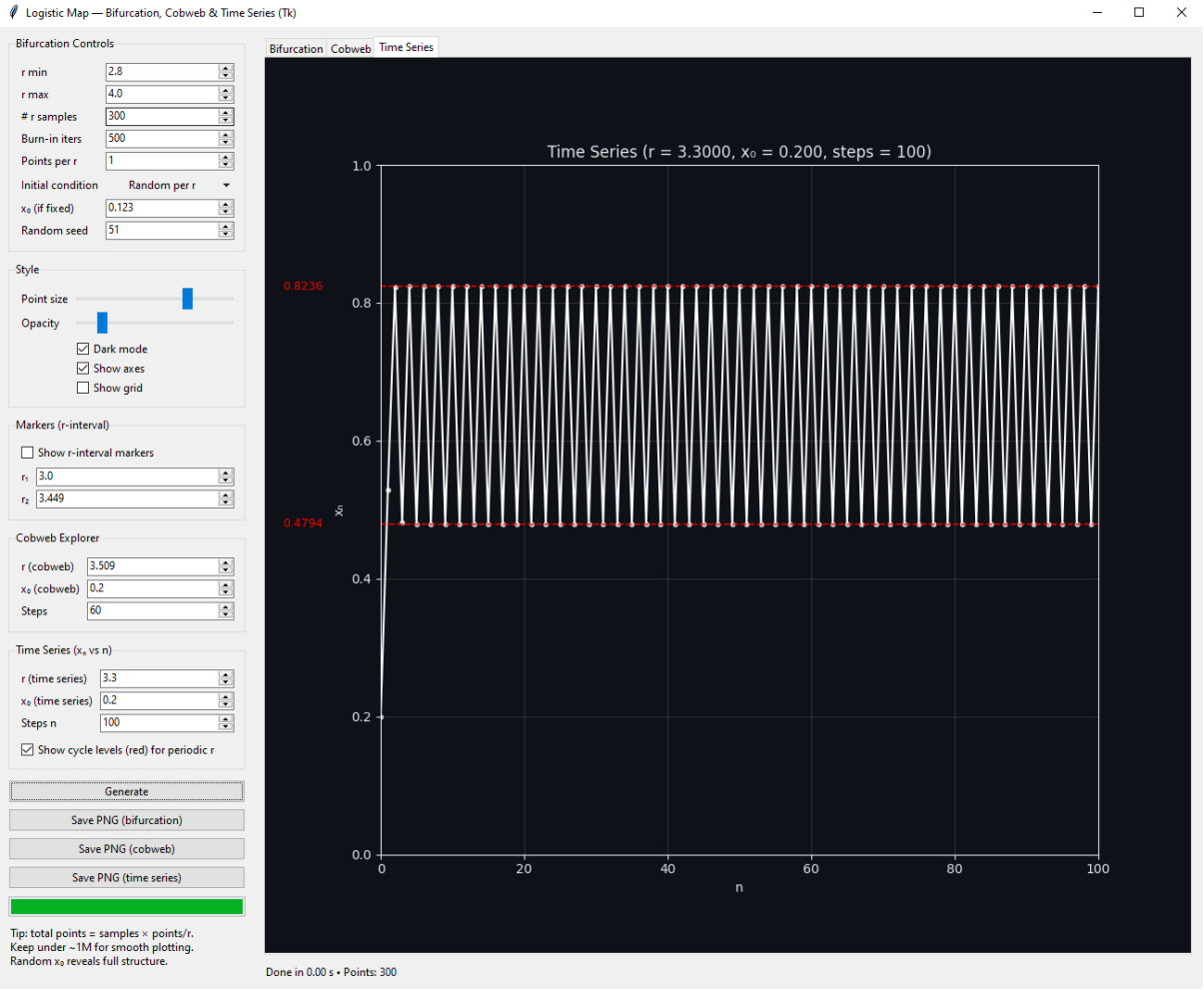

Figure 11: Screenshot of the logistic map explorer GUI, showing the evolution of the population x_n against time as steps n and parameter controls.

(iii) Cobweb Diagram Explorer

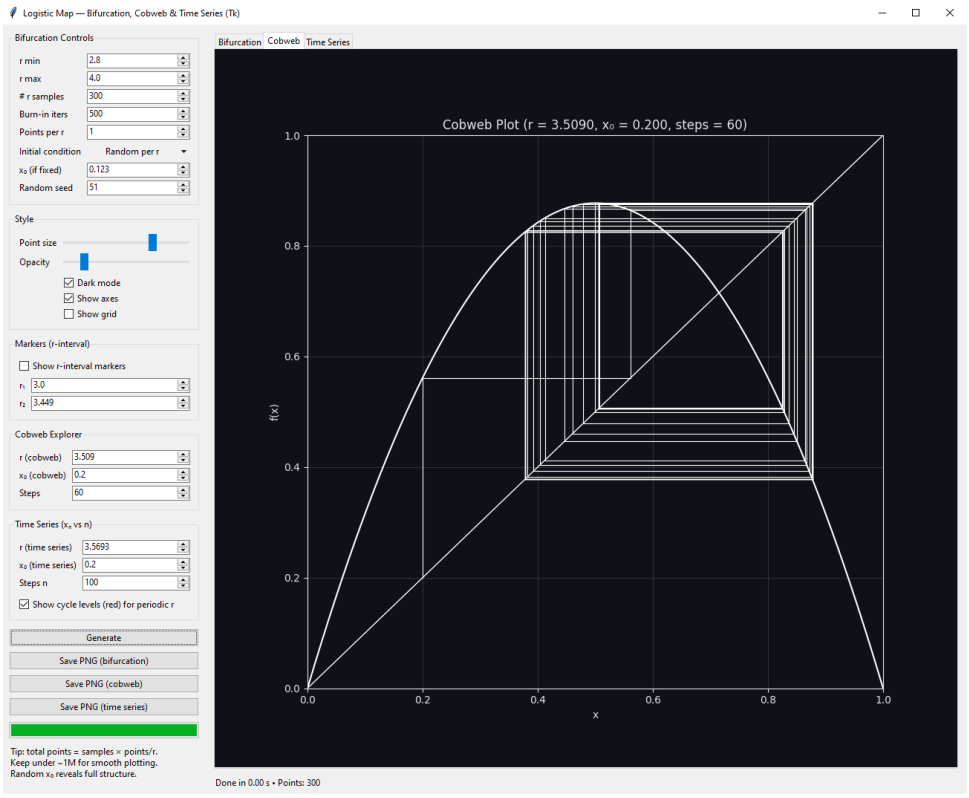

Figure 12: Screenshot of the logistic map explorer GUI, showing cobweb diagram and parameter controls.

Appendix C: Mandelbrot Explorer Interface

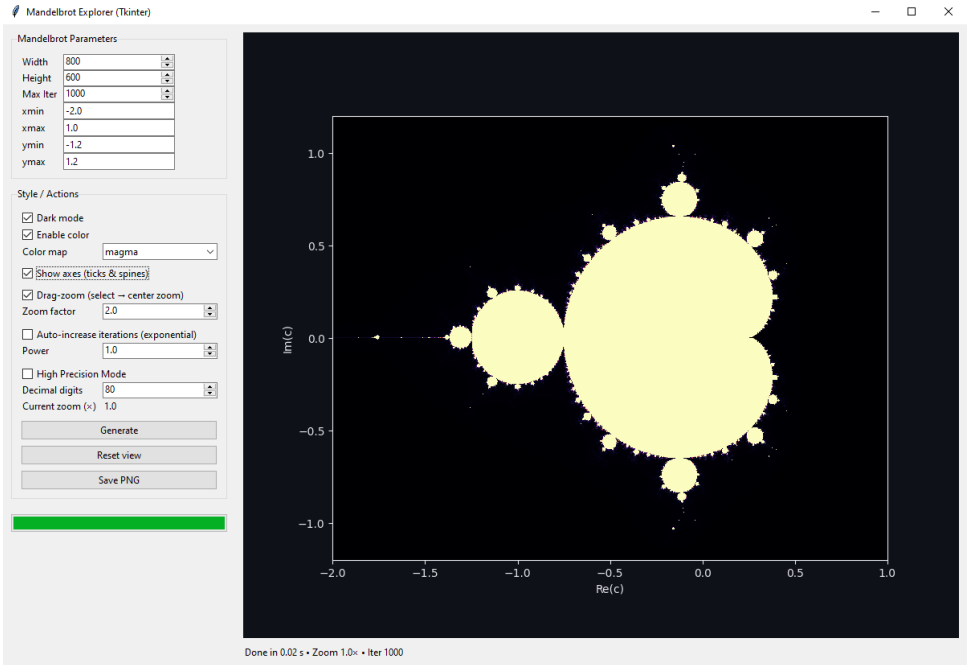

Figure 13: Screenshot of the Mandelbrot explorer GUI, showing parameter controls.

(i) Visualisation with colors

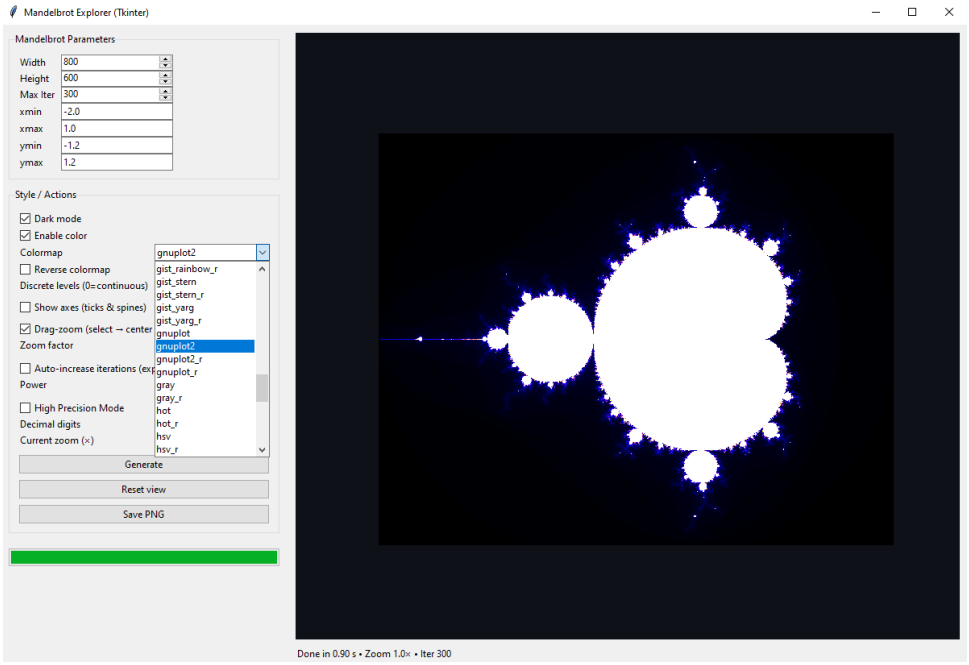

Figure 14: Screenshot of the Mandelbrot explorer GUI, showing colour controls (over 190 colours maps available).

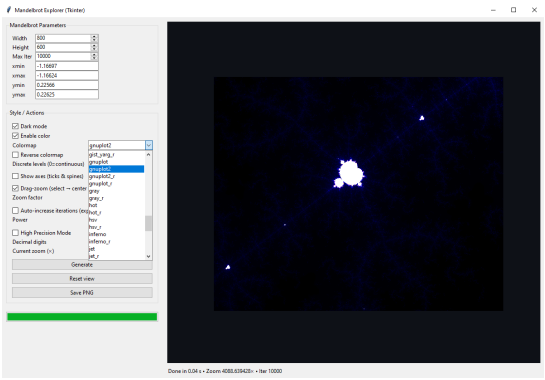

(a) Colourmap 1.

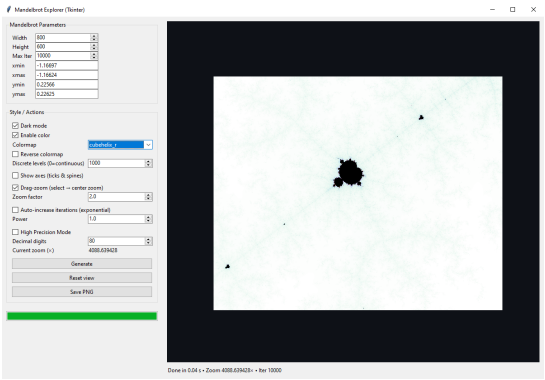

(b) Colourmap 2.

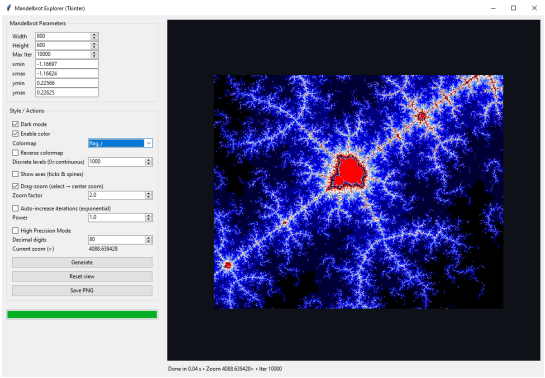

(c) Colourmap 3.

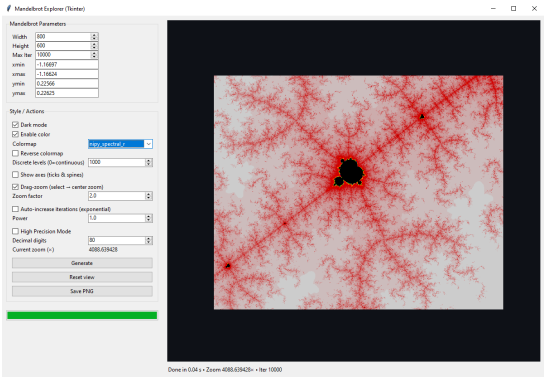

(d) Colourmap 4.

Figure 15: Screenshots of the Mandelbrot explorer GUI, showing a zoomed-in section of the set rendered under different colour maps.

(ii) Zoom system

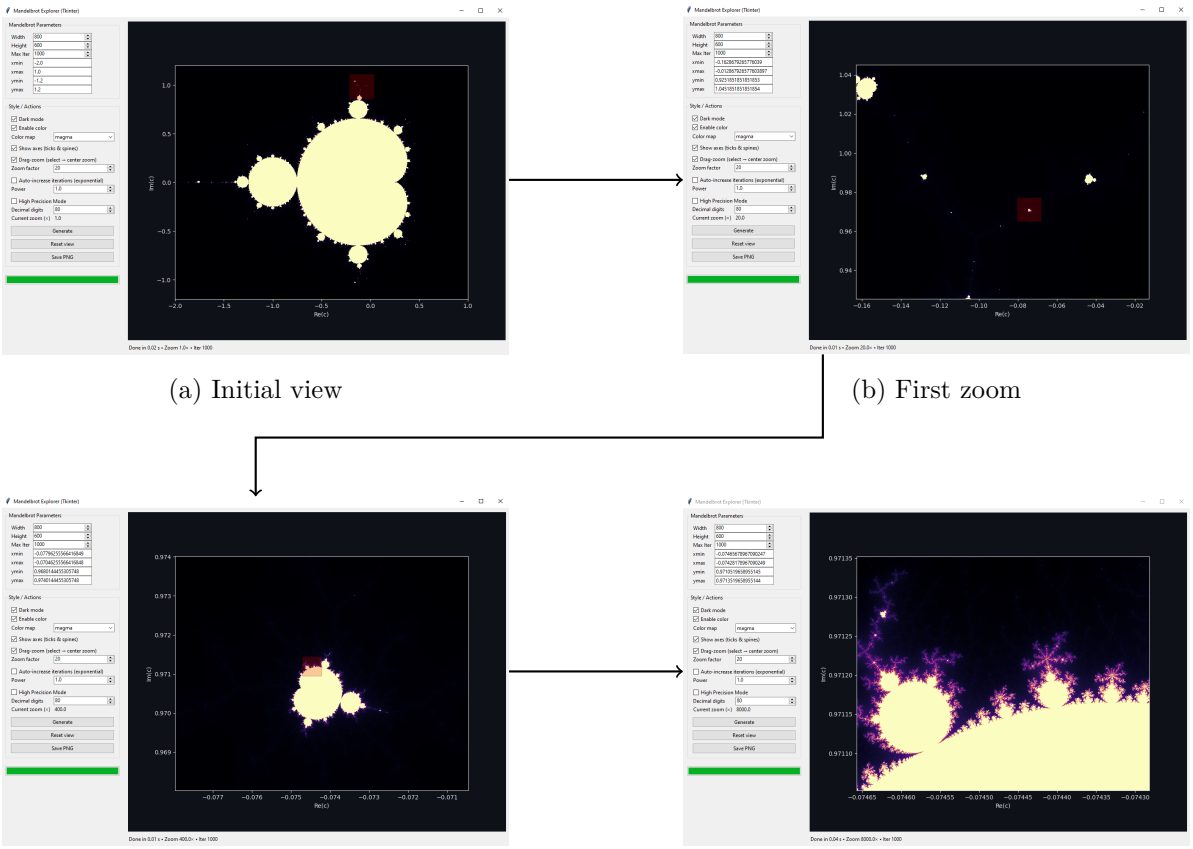

(a) Initial view

(b) First zoom

(c) Deeper zoom

(d) Deepest zoom

Figure 16: Screenshots of the Mandelbrot explorer GUI at successive zoom levels. Arrows indicate the order of magnification from (a) to (d).

Appendix D: Example Code Snippets

The following excerpts illustrate how the code generates trajectories for the logistic map and implements high-precision Mandelbrot calculations.

Logistic map iteration (Python).

```
def logistic_iter(x, r):
    return r * x * (1.0 - x)
```

Mandelbrot high-precision kernel (Python).

```
def mandelbrot_highprec(xmin, xmax, ymin, ymax, width, height, max_iter, dps):
    mp.dps = int(dps)
    image = np.zeros((height, width), dtype=np.uint16)
    ...
    return image
```